Alma Mater Studiorum · Università di Bologna

School of Universe Sciences
Department of Physics and Astronomy
Master's Degree in Astrophysics and Cosmology

Counting Primordial Perturbations Under a Corpuscular Cosmological Framework

Graduation Thesis

Presenter	Supervisor
Danielle Matlin-Wainer	Chiar.mo Prof. Roberto Casadio

Academic year [2022-2023]

Graduation date [V]

ABSTRACT

A comparative analysis of two inflationary models, semi-classical inflation and corpuscular inflation, is crucial in furthering the field of inflationary cosmology. The semi-classical model of inflation is a topic of scientific debate due to its failure to account for the quantum nature of the background or the back-reaction of perturbations on it. Corpuscular cosmology, first put forth by Dvali and Gomez, describes maximally symmetric cosmological spaces as a Bose-Einstein condensate near a point of quantum criticality. The application of this purely quantum picture to the inflationary universe allows one to recover details about this epoch that the semi-classical model leaves unaddressed. According to this model, the primordial perturbations evidenced by CMB fluctuations result from the depletion of the condensate background. The objective of this project is to derive the occupation number of depleted quanta. The significance of this value lies in its comparative potential to cosmological observables such as the CMB. The derivation of the number of primordial perturbations resulting from each inflationary de Sitter patch is reported in this paper.

Keywords: Inflation, Corpuscular Cosmology, Primordial Perturbations, Quantum Depletion

Contents

List of Figures

Chapter 1

Introduction

The inflationary epoch is a significant topic of open research in the field of cosmology because of the lack of observational constraints and theoretical limitations. This paper aims to comparatively explore the topic of inflationary perturbations as predicted by two distinct theoretical frameworks: the corpuscular cosmological model and the standard semi-classical model. These two models ascribe different physical explanations to the phenomenon of inflationary perturbations. This thesis will compare each model's predicted number of inflationary perturbations. The corpuscular model describes the inflationary phase of the universe by assuming that the background can be described as a composite of quanta akin to a Bose-Einstein condensate (Dvali and Gomez 2014). In contrast, the standard semi-classical model describes the driver of inflation as a classical field subject to quantum fluctuations. Inflationary perturbations, which go on to seed large-scale structures, are evidenced by anisotropies in the Cosmic Microwave Background (CMB). The mechanism behind the generation of these perturbations, as well as the imprint they left in the CMB, will be explored in this paper.

Corpuscular cosmology is a relatively recent theory, first put forth by Dvali and Gomez in 2011, that utilizes a fully quantum description of cosmological spaces. Therefore, its application to inflationary theory has not yet been fully realized. Further computations are needed to quantify inflationary perturbations under a corpuscular framework. This thesis aims to compute the predicted number of primordial perturbations in the universe at the end of inflation. One significant aspect of this computation is its connection to the CMB. This project will allow for a comparison between the corpuscular model and cosmological observations and will, therefore, corroborate the viability of the corpuscular model observationally.

This paper will briefly explain the Cosmic Microwave Background, a relic radiation from the last scattering surface. The CMB is a key inflationary observable; thus, it is important to discuss its origin and features. The anisotropies of the CMB temperature spectrum are perhaps its most informative feature, as they can be traced

to density fluctuation in the early universe. As such, this paper will discuss their formation and the statistical tools used to analyze them. This will be followed by an introduction to cosmological models and the necessity of an inflationary epoch. Subsequently, this paper will explain the standard semi-classical inflationary theory, which posits that the universe underwent a rapid exponential expansion in the first fraction of a second after the Big Bang. Inflation can be described by a Slow-Roll model. This model posits that inflation is driven by a scalar field known as the inflaton, whose potential determines the rate of expansion. The governing equations of this model and the conditions required for the inflaton will be discussed.

The following chapter will discuss inflationary perturbations under a semi-classical model. The inflaton exhibits quantum fluctuations that are stretched to classical scales by the universe's rapid expansion. These quantum fluctuations become the density perturbations and seed the large-scale structures in the universe today. An important concept in understanding inflationary perturbations is the evolution of the Hubble horizon during this period. The Hubble horizon marks the distance objects can be observed or the extent of causal contact. The universe's rapid expansion causes the co-moving Hubble horizon to shrink during inflation. As a result, quantum fluctuations are stretched to scales much larger than the Hubble horizon. These fluctuations become 'frozen' when they exit the horizon, i.e., they cannot propagate, as they are no longer subject to causal processes. After inflation has ended, the universe transitions to a decelerating expansion, causing the horizon to grow. Therefore, the quantum fluctuations re-enter the horizon at a later epoch as classical perturbations, seeding CMB anisotropies and forming large-scale structures (Baumann 2012).

Special attention will then be given to the statistical analysis and quantification of these perturbations. Perturbation theory assesses the impact of small perturbations in the early universe on cosmological observables. The most significant statistical tool in analyzing these perturbations is their power spectrum. Additionally, as these perturbations originate as quantum fluctuations, a quantum framework is needed to conduct an accurate statistical analysis. A possible particularly significant inflationary phase in the generation of perturbations is the ultra-slow roll phase in which the number of perturbations grows exponentially (Ballesteros et al. 2020b). The dynamics of the phase will be outlined, and this semi-classical ultra-slow roll model will be used to compute the expected number of inflationary perturbations.

The semi-classical model of inflation is limited by its inability to account for the quantum nature of the background and the back-reaction of perturbations on it. The corpuscular picture aims to utilize a purely quantum description to explain inflationary dynamics and the production of primordial perturbations. This theory was first put forth to describe black holes as a Bose-Einstein condensate of

gravitons at a critical point with gapless degenerate Bogoliubov modes (Dvali and Gomez 2011). A crucial property of Bose-Einstein condensates is that they undergo a process known as depletion in which quanta are emitted, and the background loses energy. This picture can be extended beyond black holes and applied to all maximally symmetric spaces, such as the universe during inflation. In this scenario, inflationary dynamics, given by the Friedmann equations or the expansion rate given by the Hubble parameter, can be recovered from the energy density of gravitons. During inflation, graviton interaction causes the quanta to deplete or get 'squeezed out' of the ground state and become propagating perturbations (Dvali and Gomez 2014). Therefore, according to this theory, the primordial perturbations evidenced by the CMB should correspond to the amount of quanta depleted by the condensate. However, it is important to note that this picture holds inside each individual de Sitter patch. The perturbations imprinted on the CMB spectra can be recovered by multiplying the predicted number of depleted quanta by the number of Hubble patches present in the universe during inflation.

This thesis aims to compute the occupation number of depleted quanta during inflation according to a corpuscular cosmological model. It will begin by explaining the current understanding of the inflationary epoch, its observational tracers, and how it fits into modern cosmological models. An in-depth discussion of inflationary models and the statistical properties of inflationary perturbations will be analyzed under a semi-classical framework. A derivation of the occupation number of primordial perturbations using quantum field theory will be provided. Subsequently, the corpuscular model will be explored, briefly explaining its initial application to black holes, followed by its assessment of inflationary cosmology. Lastly, the derivation of the occupation number of depleted quanta, a discussion of its physical interpretation, and a comparison to the quantum field theory result will be provided.

Chapter 2

Inflationary Cosmology

This chapter will explore the period of inflation under a semi-classical cosmological model. The chapter begins by discussing a key inflationary observable, the CMB, explaining its formation and the information it carries. The Hot Big Bang model and its limitations will be introduced, including the horizon, flatness, and monopole problems. The solution to these limitations will also be addressed: a period of rapid accelerated expansion known as inflation. Subsequently, the dynamics of inflation and the conditions it must meet will be explored, specifically the theory of slow-roll inflation.

2.1 The Cosmic Microwave Background

This section will discuss the formation of the Cosmic Microwave Background (CMB) and the cosmological information it holds. Recombination, the last scattering surface, and the formation of the CMB will be explained. The temperature map of the CMB reveals a homogeneous isotropic universe with several small anisotropies. The progenitors of these anisotropies are multifaceted, but they can be traced back to primordial density fluctuations. Therefore, these temperature fluctuations can be analyzed to study the primordial universe. The greatest tool in this analysis is the power spectrum of temperature anisotropies.

2.1.1 Recombination and the Last Scattering Surface

The Cosmic Microwave Background (CMB) is the earliest piece of observational evidence present in the universe, and it is one of the few tools available for cosmologists to learn about the inflationary era. The CMB is a nearly uniform background radiation that permeates the entire universe and is observable in the microwave spectrum. It is a relic radiation from the early universe, providing a snapshot of the universe at the redshift of last scattering, $z_{ls} \approx 1100$. Not long before this, 380,000 years after the Big Bang, a phenomenon known as recombination occurred at a redshift

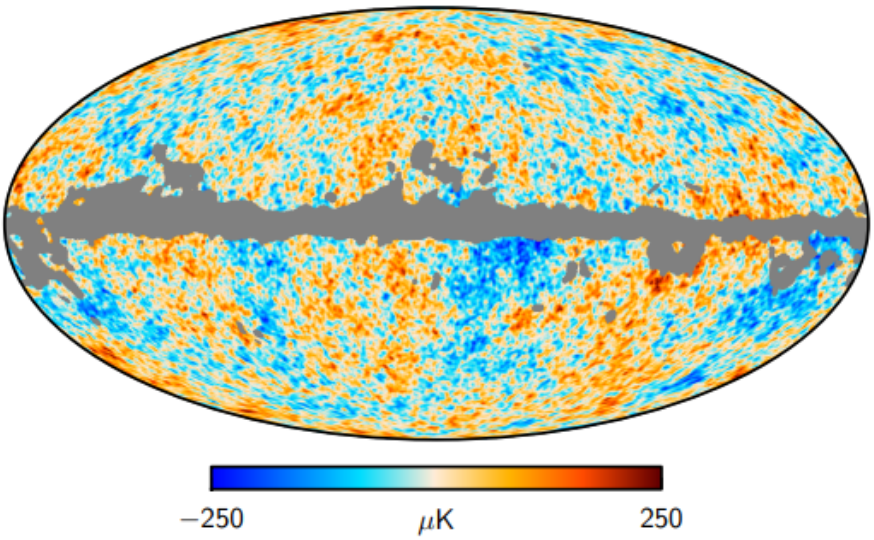

Figure 2.1: 2018 Planck findings report the CMB temperature map generated by the Commander component separation algorithm. The map is smoothed to a 60° FWHM resolution, with the grey areas indicating the masked regions used in the analysis, retaining 86% of the sky. The dipole moment, $\ell = 1$, is masked to avoid Milky Way contamination (Akrami et al. 2020).

of $z_{rec} \approx 1500$. Before this event, the universe was a hot, dense, opaque plasma, as photons were subject to frequent Thompson scatters. As the universe cools over time, recombination marks when it is cold enough for protons and electrons to combine into neutral hydrogen atoms. At this moment, photons decoupled from matter as they could freely travel without being scattered by free electrons. This transition marks the moment when the universe became transparent to radiation. Naturally, this is a gradual process; not every photon could travel freely at the exact moment when the first neutral hydrogen atom formed, hence the discrepancy between the last scattering event at z_{ls} and z_{rec}. The photons that escaped at the last scattering constitute the CMB. Therefore, the temperature map provided by CMB radiation reflects a snapshot of the universe at z_{ls} and any fluctuations reflected in this temperature map can be related to perturbations in the universe resulting from inflation (Coles and Lucchin 2002).

2.1.2 CMB Anisotropies

The average temperature of the black-body spectrum of the CMB has been measured as (Fixsen 2009),

$$T_{CMB} = 2.72548 \pm 0.00057K. \tag{2.1}$$

The temperature map of the CMB illustrated by Figure 2.1 depicts a broadly homogeneous and isotropic universe containing small fluctuations that differ from the average value by approximately 10^{-5} (Aghanim et al. 2020). The progenitors of the

anisotropies are multifaceted and can be broken down into two categories: primary anisotropies, which reflect the conditions of the cosmic fluid at the moment of last scattering, and secondary anisotropies, which reflect processes the CMB photons undergo as they travel towards Earth. There are three sources of primary anisotropies: effects relating to gravity, density, and velocity. The gravitational effects can be summarized as follows: if a CMB photon is located in a potential well at z_{ls}, it will expend energy to escape the potential well and thus be redshifted; likewise, the CMB photon would be blueshifted if it were to enter a potential well. Additionally, given adiabaticity, overdense regions lead to particle heating, and underdense regions lead to particle cooling; therefore, density fluctuations result in temperature fluctuations. These two phenomena work simultaneously and have opposing effects. The combined effect, the Sachs-Wolfe effect, indicates that overdensities correspond to temperature fluctuations below T_{CMB}, while underdensities correspond to temperature fluctuations above T_{CMB}. CMB photons are also subject to the Doppler effect and will be red or blueshifted depending on their velocity relative to us. There are also several different types of secondary anisotropies. CMB photons are also subject to falling into or escaping potential wells on their path to Earth; the Integrated Sachs Wolfe effect accounts for this. CMB photons can also be deflected when traveling near massive objects, or they could gain or lose energy when passing through ionized mediums. However, these anisotropies can be considered white noise for cosmological studies or, more specifically, studying the inflationary epoch.

While the Sachs-Wolfe effect dominates CMB anisotropies on large angular scales, CMB anisotropies are dominated by acoustic oscillations on small angular scales. These acoustic oscillations resulted from density perturbations that 'froze' outside the cosmological horizon during inflation. After inflation, these density perturbations re-entered the horizon during the radiation-dominated era when matter and radiation were coupled. These fluctuations led to the production of sound waves that filled the early universe. In overdense regions, gravitational forces led to the compression of the cosmic fluid, and radiative pressure acted as a restoring force, causing the fluid to rebound, thus generating acoustic oscillations. These sound waves were imprinted in the CMB as a pattern of temperature and density fluctuations observed as a series of acoustic peaks. In summation, CMB anisotropies are explained mainly by the Sachs-Wolfe effect on large angular scales and acoustic oscillations on small angular scales. Both progenitors result from primordial density perturbations. Therefore, CMB anisotropies can be used to probe such perturbations.

2.1.3 Power Spectrum

The power spectrum of CMB fluctuations is the most significant statistical tool used to analyze and quantify these perturbations. The power spectrum is a plot of

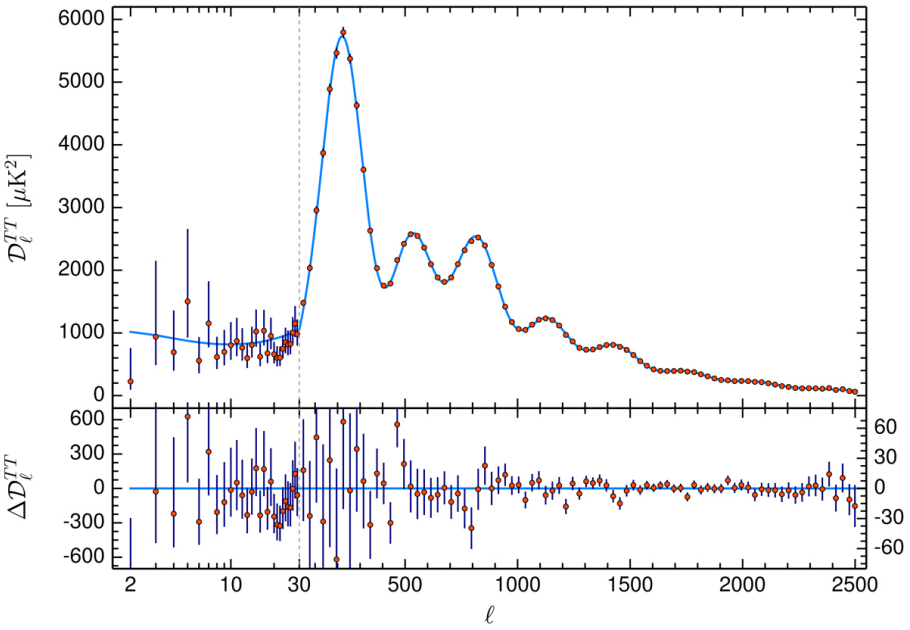

Figure 2.2: Temperature power spectrum of the CMB as observed by Planck 2018. The high-multipole range ($\ell \geq 30$) shows the combined frequency temperature spectrum. The low-multipole range ($2 \leq \ell \leq 29$) presents the power spectrum from the Commander component-separation algorithm, covering 86% of the sky. The light blue curve represents the best-fit base-ΛCDM theoretical spectrum. The lower panel displays residuals relative to this model. Error bars indicate $\pm 1\ \sigma$ uncertainties, including cosmic variance, but excluding foreground model uncertainties at $\ell \geq 30$. Note the shift from logarithmic to linear scaling at $\ell = 30$ (Aghanim et al. 2020).

temperature anisotropies as a function of angular scale, or equivalently, multipole moment, ℓ, which is inversely proportional to angular scale. This spectrum can be visualized by Figure 2.2, which presents the findings from Aghanim et al. 2020. This power spectrum holds much information about the early universe and is a crucial probe of inflationary models. For example, at large scales, low ℓ, the power spectrum can indicate the amplitude and distribution of large-scale density fluctuations. At smaller scales, larger ℓ, the height and spacing of acoustic peaks indicate baryonic and dark matter densities at that time, and the position of the first acoustic peak indicates the scale of last scattering. These findings have a profound impact on early universe models. The observed size of the last scattering is smaller than the extent of homogeneity indicated by the CMB temperature map, Figure 2.1. Additionally, the CMB findings indicate a flat universe, corresponding to $\Omega_{tot} \approx 1$, which requires fine-tuning initial conditions. The discovery of the CMB revealed multiple problems with early universe models that an inflationary epoch can solve (Coles and Lucchin 2002). These problems and their solutions will be discussed in the next sections.

Lastly, the scale dependence of the power spectrum, given by its spectral index, n_s, is an important probe of inflationary models. Inflation predicts a nearly scale-invariant power spectrum; CMB data indicates $n_s \approx 0.96$ (Aghanim et al. 2020).

This value indicates a slight red tilt; larger scale perturbations have slightly greater amplitudes. Therefore, any inflationary model must be able to produce nearly scale-independent perturbations whose amplitudes corroborate the amplitude of the power spectrum.

2.2 The Hot Big Bang Model

This section introduces the standard cosmological model used to describe the universe's evolution, the Hot Big Bang model. The equations governing the dynamics and geometry of the universe will be explored. This model has three significant problems that require an inflationary epoch to solve. Firstly, the observed flatness of the universe requires a fine-tuning of initial conditions. Additionally, the homogeneity observed by the CMB is greater than the extent of causal contact. Lastly, GUT theories indicate the presence of magnetic monopoles that have never been observed.

2.2.1 Cosmological Models

One of the most widely studied cosmological models is the Hot Big Bang model, which describes a universe that originates from an initial singularity and expands over time. A core tenet of this model is the cosmological principle, which theorizes that the universe is homogeneous and isotropic. This theory describes the universe's entire history, including inflation, cooling, nucleosynthesis, and the formation of large-scale structures; however, this paper focuses on its description of inflation. It assumes that all matter in the universe can be broken down into three components. Baryonic matter makes up 4% of all matter; dark matter makes up 26%, and dark energy, which is accounted for by the cosmological constant and explains the universe's accelerated expansion, makes up the remaining 70%. According to this model, the geometry of the universe can be described by the FLRW metric,

$$ds^2 = -c^2dt^2 + a^2\left(\frac{dr^2}{1-kr^2} + r^2(d\theta^2 + \sin^2\theta\, d\phi^2)\right). \tag{2.2}$$

In this equation, ds^2 represents the spacetime interval, $a = a(t)$ is the scale factor, a dimensionless quantity that describes how distances between two points in the universe change as a function of time, k represents the curvature parameter: a hyperbolic or open universe is given by $k = -1$, a flat universe is given by $k = 0$, and a spherical or closed universe is given by $k = 1$, r, θ and ϕ are comoving coordinates, and c is the speed of light, which is often set to 1.

Using the FLRW metric and Einstein's field equations, one can derive the Friedmann equations, describing the dynamics of the universe,

$$H^2 = \frac{8\pi G}{3}\rho - \frac{kc^2}{a^2} + \frac{\Lambda c^2}{3}, \tag{2.3}$$

$$\frac{\ddot{a}}{a} = -\frac{4\pi G}{3}\left(\rho + \frac{3p}{c^2}\right) + \frac{\Lambda c^2}{3}. \tag{2.4}$$

H is the Hubble parameter, which accounts for the rate of expansion in the universe and is defined as,

$$H(t) \equiv \frac{\dot{a}}{a}. \tag{2.5}$$

In the above equations, ρ defines the universe's energy density, p is the pressure, Λ is the cosmological constant, and G is the gravitational constant. The dots indicate derivatives with respect to time (Coles and Lucchin 2002).

The first Friedmann equation describes the time evolution of the scale factor given the energy density and curvature of the universe; the second equation probes whether the universe's expansion is accelerated or decelerated. These equations can be solved for different epochs or different types of universes. For example, suppose one considers a matter, or dust, dominated universe, a radiation-dominated universe, or a dark-energy-dominated universe. In each case, findings can be made concerning how various cosmological parameters relate to one another or depend on time. Solutions to the Friedmann equations for three different cosmological epochs, matter-dominated, radiation-dominated, and dark-energy-dominated, are detailed below.

$$a = \begin{cases} a_{\text{dust}} \sim t^{2/3} & \text{for } H^2_{\text{dust}} \sim \rho_{\text{dust}} \sim a^{-3}_{\text{dust}} \sim t^{-2} \\ a_{\text{rad}} \sim t^{1/2} & \text{for } H^2_{\text{rad}} \sim \rho_{\text{rad}} \sim a^{-4}_{\text{rad}} \sim t^{-2} \\ a_{\Lambda} \sim e^{H_{\Lambda} t} & \text{for } H^2_{\Lambda} \sim \rho_{\Lambda} \sim \Lambda/3 \end{cases}, \tag{2.6}$$

$$p = \begin{cases} a_{\text{dust}} \sim 0 \\ a_{\text{radiation}} \sim \rho/3 \\ a_{\Lambda} \sim -\rho \end{cases}. \tag{2.7}$$

Another cosmological parameter crucial to the Friedmann models is the density parameter,

$$\Omega = \frac{\rho}{\rho_c}, \tag{2.8}$$

where ρ_c is the critical density, the energy density at which the universe would be flat; it is defined as,

$$\rho_c = \frac{3H^2}{8\pi G}. \tag{2.9}$$

If the universe's density exceeds the critical density, the universe is closed. Conversely, the universe is open if the universe's density is less than the critical density.

One can rewrite the Friedman equations to relate the curvature parameter to the density parameter,

$$\Omega - 1 = \frac{kc^2}{a^2H^2}. \tag{2.10}$$

Thus, the different scenarios of universe geometries can be summarized as follows:

- Open Universe: $0 < \Omega < 1$, $k < 0$, $\rho < \rho_c$.
- Flat Universe: $\Omega = 1$, $k = 0$, $\rho = \rho_c$.
- Closed Universe: $\Omega > 1$, $k > 0$, $\rho > \rho_c$.

Current cosmological findings indicate that the density parameter today has a value of,

$$\Omega_0 = 1.0007 \pm 0.0037, \tag{2.11}$$

indicating a nearly flat universe. This leads one to the first shortcoming of the Hot Big Bang model (Vazquez Gonzalez, Padilla, and Matos 2020).

2.2.2 Flatness Problem

The flatness problem arises from the observation that the universe appears to be exceedingly close to flat on large scales; precise measurements of the CMB and the distribution of galaxies corroborate this. Guth first formulated this problem in his 1981 paper, 'Inflationary Universe: A Possible Solution to the Horizon and Flatness Problems.' Today's flatness indicates that the universe's density is extremely close to the critical value. In a closed universe, gravitational forces exerted by the matter and energy contents of the universe cause the expansion to eventually reverse, leading to a cosmic collapse known as the 'Big Crunch.' This collapse would have occurred on the order of Planck time. Conversely, in an open universe, expansion continues indefinitely as the density dwindles to a value below ρ_c until the universe becomes a cold, dark, inert place known as the 'Big Freeze' or 'Heat death.' For a universe to stably evolve until the present day, it must be consistently flat; in other words, its density must be approximately equal to the critical density throughout its evolution. However, this condition raises complications: curvature conservation dictates that if the universe at any point deviated from flatness, this deviation would compound in time and lead to a universe with curvature. Therefore, this flatness condition can only be maintained by an extreme fine-tuning of ρ and H. Assuming the temperature after the Plank era was 10^{15}GeV, the Hubble parameter must not be adjusted by one part in 10^{60}. In other words, the density of the universe must be fine-tuned such that it satisfies the following condition:

$$\frac{\rho - \rho_c}{\rho} < 10^{-60}. \tag{2.12}$$

Any deviation from this would result in an open or closed universe. Such an extreme fine-tuning of initial conditions seems unnatural and led Guth to conclude that an additional cosmological phenomenon, known as inflation, is needed to explain the observed flatness in the universe (Guth 1981).

2.2.3 Horizon Problem

The flatness problem was not the only issue Guth took with the Hot Big Bang model that required an inflationary solution. Guth also found that this model required the early universe to violate causality. CMB observations have indicated that the universe is homogeneous and isotropic. This thermal equilibrium condition indicates that the thermalized regions are in, or have been in, causal contact with one another. However, Guth found that there are 10^{83} casually disconnected regions that satisfy this homogeneity condition, thus violating causality. Guth found this finding by comparing the particle horizon, $l(t)$, to the radius that will evolve into the observable universe, $L(t)$. The particle horizon is the maximum distance from which light could have traveled since the beginning of the universe, and it can be defined as,

$$l(t) = a(t) \int_0^t \frac{dt'}{a(t')} = 2t. \tag{2.13}$$

$L(t)$ can be found by the conservation of entropy,

$$L(t) = \left[\frac{s_p}{s(t)}\right]^{1/3} L_p, \tag{2.14}$$

where s_p is the current entropy density of the universe, and L_p is the radius of the currently observable universe. The ratio of the two volumes is,

$$\frac{l^3(t)}{L^3(t)} = 4 \cdot 10^{-89} \cdot \mathcal{R}^{-1/2} \left(\frac{M_{Pl}}{T}\right)^3, \tag{2.15}$$

where, $\mathcal{R}$ is the number of effective degrees of freedom, T is the temperature of the universe, and M_{Pl} is the Planck mass. These values can be defined in the early universe where $\mathcal{R} \approx 100$ and $T_0 = 10^{17}$Gev. Therefore, the ratio between the scale of the particle horizon at this time, l_0, and the scale of the universe that would need to be causally connected to produce a homogeneous universe, L_0, can be written as,

$$\frac{l_0^3}{L_0^3} = 10^{-83}. \tag{2.16}$$

The scale of the observable universe was 10^{83} times larger than the scale of the particle horizon at this time, indicating 10^{83} causally disconnected patches in the universe today (Guth 1981). The corpuscular interpretation of l_0 will be discussed in Chapter 5. In short, the Horizon problem is the issue of not having enough time for the universe to thermalize on the scales indicated by the CMB.

2.2.4 Magnetic Monopole Problem

In 1974, Georgi and Glashow developed Grand Unified Theories (GUT), which unify three of the four fundamental forces described by the Standard Model of particle physics: strong, weak, and electromagnetic. These theories assert that a unified or symmetric phase existed at temperatures of $T_{GUT} \approx 10^{32}$ K in the early universe. As the universe evolved and its temperature decreased, it underwent various phase transitions until reaching the symmetries described by the Standard Model of particles, recovering the matter observed in the universe today. These phase transitions generate topological defects depending on the type of symmetry-breaking and the dimension the transition is characterized by. Magnetic monopoles are expected to emerge as a consequence of zero-dimensional symmetry breaking. The non-relativistic characteristic of monopoles predicts an extremely high number density of magnetic monopoles at the time of symmetry breaking. In other words, the universe should be dominated by magnetic monopoles. Furthermore, this abundance of magnetic monopole indicates a density parameter greater than 1, leading to a closed universe. However, this has been refuted by observations. Additionally, no monopoles have ever been observed, hence the Magnetic Monopole Problem (Vazquez Gonzalez, Padilla, and Matos 2020).

2.3 Inflation

This section will introduce the inflationary epoch, a period of rapid expansion that solves the issues with the Hot Big Bang model. In order to solve the flatness, horizon, and monopole problems, inflation must last sufficiently long. The inflationary field, known as the inflaton, must slowly roll down an almost flat potential to satisfy this condition. The slow-roll parameters ϵ and η can account for these conditions, which must be less than one throughout inflation. The explicit formulation of these conditions and their impact on inflationary dynamics will be discussed.

2.3.1 The Inflationary Solution

These issues with the Hot Big Bang model can be accounted for by including a period in which the universe underwent accelerated expansion in a mere fraction of a second, known as inflation. During this period the scale factor and the Hubble parameter can be described by:

$$\ddot{a} > 0, \tag{2.17}$$

and,

$$\frac{d}{dt}\left(\frac{1}{aH}\right) < 0. \tag{2.18}$$

The first equation indicates the accelerated expansion of the universe. The second equation indicates that the observable universe shrinks during inflation, as $(1/aH)$ corresponds to the comoving Hubble length. These conditions, in conjunction with the Friedmann equations, implies,

$$(\rho + 3p) < 0. \tag{2.19}$$

As ρ is always considered to be a positive quantity, the inflationary universe is characterized by a negative pressure,

$$p < -\frac{\rho}{3}. \tag{2.20}$$

One can now explore how an inflationary period can solve the problems with the Hot Big Bang model. To begin this analysis, assume a universe with a cosmological constant, Λ, is a perfect fluid with the following state equation,

$$p = -\rho. \tag{2.21}$$

A de Sitter model most commonly describes the inflationary epoch. The de Sitter universe is a single-component universe that contains only vacuum energy, without matter or radiation. It is characterized by a positive cosmological constant, the following scale factor, and constant Hubble parameter,

$$a(t) \propto e^{Ht}, \tag{2.22}$$

$$H = \sqrt{\frac{\Lambda}{3}}. \tag{2.23}$$

The issue of the observed flatness of the universe can be explained by analyzing the behavior of the density parameter during this inflationary period. An accelerated expansion indicates that $1/(aH)$ decreases with time; therefore, by equation (2.10), the density parameter approaches unity rather than diverging from it. Now, the question is to quantify the required magnitude of this expansion. Assuming inflation begins at $t = t_i$ and ends at $t = t_f$ one finds,

$$|\Omega - 1|_{t=t_f} \approx 10^{-60}. \tag{2.24}$$

The effect of inflation on the density parameter is given by quantifying the ratio of the density parameters at the beginning and end of inflation,

$$\frac{|\Omega - 1|_{t=t_f}}{|\Omega - 1|_{t=t_i}} = \left(\frac{a_i}{a_f}\right)^2 \equiv e^{-2\mathcal{N}}. \tag{2.25}$$

Thus, introducing the number of e-folding, $\mathcal{N}$, quantifying the number of times the scale factor grows by a factor of e during inflation. It can be more formally defined as,

$$\mathcal{N} = \ln\left(\frac{a_f}{a_i}\right). \tag{2.26}$$

Therefore, the number of e-folds, $\mathcal{N}$, must be greater than 60 to reproduce the value of the density parameter measured today and solve the flatness problem. In summation, the universe's rapid expansion magnified the curvature radius such that, locally, the universe appears spatially flat.

The horizon problem can be solved by this inflationary period as well. The universe rapidly expands during this period, and the comoving Hubble horizon shrinks, according to (2.18). As a result, a region of size l_0, given by (2.16), was stretched to constitute the observable universe today. Within the Hubble horizon initially, this region was stretched to superhorizon scales, making it appear causally disconnected. Therefore, according to CMB observations, the causally disconnected regions in thermal equilibrium were in causal contact before inflation. Thus, homogeneity can be recovered without violating causality, and the horizon problem is solved.

The monopole problem can also be solved by this period of rapid expansion. The drastic inflationary expansion diluted the universe's contents at the beginning of inflation, ensuring that these monopoles were insignificant in the observable universe. Therefore, the inflationary epoch can explain why no magnetic monopoles have ever been detected despite the universe being once dominated by them (Vazquez Gonzalez, Padilla, and Matos 2020).

2.3.2 Slow-Roll Inflation

Inflation is a very crucial yet peculiar cosmological phenomenon. This section will explore the dynamics of inflation and the conditions it must satisfy. The most widely accepted inflationary models describe the driver of inflation as a single scalar field, ϕ, known as the inflaton, which parametrizes the evolution of the inflationary energy density. The following action can describe the dynamics of this field,

$$S = \int d^4x\sqrt{-g}\left(\frac{1}{2}R + \frac{1}{2}g^{\mu\nu}\partial_\mu\phi\partial_\nu\phi - V(\phi)\right) = S_{EH} + S_\phi, \tag{2.27}$$

where R is the Ricci scalar, $V(\phi)$ is the inflaton potential, S_{EH} is the Einstein-Hilbert action, and S_ϕ is the matter action. The corresponding energy-momentum tensor can be defined as,

$$T_{\mu\nu}(\phi) \equiv -\frac{2}{\sqrt{-g}}\frac{\delta S_\phi}{\delta g^{\mu\nu}} = \partial_\mu\phi\partial_\nu\phi - g_{\mu\nu}\left(\frac{1}{2}\partial^\sigma\phi\partial_\sigma\phi + V(\phi)\right). \tag{2.28}$$

The equation of motion of the inflaton is found by varying the action,

$$\frac{\delta S_\phi}{\delta\phi} = \frac{1}{\sqrt{-g}}\partial_\mu\left(\sqrt{-g}\partial^\mu\phi\right) + V_{,\phi} = 0, \tag{2.29}$$

where $V_{,\phi} \equiv dV/d\phi$. Considering the FLRW metric for a homogeneous scalar field, one can assume the scalar energy-momentum tensor is that of a perfect fluid with,

$$p_\phi = \frac{1}{2}\dot{\phi}^2 - V, \tag{2.30}$$

and,

$$\rho_\phi = \frac{1}{2}\dot{\phi}^2 + V, \tag{2.31}$$

where the state equation is defined as,

$$w_\phi \equiv \frac{p_\phi}{\rho_\phi}. \tag{2.32}$$

Therefore, the inflationary conditions of negative pressure, i.e., $w_\phi < 0$, and accelerated expansion, $w_\phi < -1/3$, can be given by a scalar field if its potential energy dominates over its kinetic energy,

$$V \gg \frac{1}{2}\dot{\phi}. \tag{2.33}$$

This is known as the slow-roll condition because it indicates that the inflaton must slowly roll down an almost flat potential (Baumann 2012).

The following equations of motion give the dynamics of the inflaton and its geometry,

$$\ddot{\phi} + 3H\dot{\phi} = -V_{,\phi} \tag{2.34}$$

where,

$$H^2 = \frac{1}{3}\left(\frac{1}{2}\dot{\phi}^2 + V(\phi)\right). \tag{2.35}$$

It is useful to introduce the two slow-roll parameters, ϵ, and η, to describe the inflationary dynamics. The second Friedmann equation can be written as,

$$\frac{\ddot{a}}{a} = -\frac{1}{6}(\rho_\phi + 3p_\phi) = H^2(1-\epsilon), \tag{2.36}$$

where,

$$\epsilon \equiv \frac{3}{2}(w_\phi + 1) = \frac{1}{2}\frac{\dot{\phi}^2}{H^2}. \tag{2.37}$$

ϵ can be related to the evolution of the Hubble parameter by,

$$\epsilon = -\frac{\dot{H}}{H^2} = -\frac{d\ln H}{d\mathcal{N}}, \tag{2.38}$$

where $d\mathcal{N} = Hdt$. The slow-roll parameter ϵ describes the rate at which the inflaton's potential energy dominates over its kinetic energy. Accelerated expansion occurs when ϵ is much less than 1 and ends when $\epsilon = 1$. In fact, $p_\phi \to -\rho_\phi$, as $\epsilon \to 0$. These conditions for epsilon are met when (2.33) is satisfied.

Furthermore, this accelerated expansion must hold for a sufficiently long time, requiring the second time derivative of the inflaton to satisfy,

$$|\ddot{\phi}| \ll |3H\dot{\phi}|, \tag{2.39}$$

and

$$|\ddot{\phi}| \ll |V_{,\phi}|. \tag{2.40}$$

This leads one to the second slow-roll parameter, η, which also must be much less than one to satisfy the above condition. It describes the curvature of the inflaton potential along the inflaton field direction and is given by,

$$\eta = -\frac{\ddot{\phi}}{H\dot{\phi}} = \epsilon - \frac{1}{2\epsilon}\frac{d\epsilon}{dN}. \tag{2.41}$$

The slow-roll parameters can also be written in terms of the inflaton potential, known as the potential slow-roll parameters,

$$\epsilon_v(\phi) \equiv \frac{M_{\rm Pl}^2}{2}\left(\frac{V_{,\phi}}{V}\right)^2, \tag{2.42}$$

$$\eta_v(\phi) \equiv M_{\rm Pl}^2\frac{V_{,\phi\phi}}{V}. \tag{2.43}$$

The Planck mass is included here to ensure that the slow-roll parameters are dimensionless; however, it can be set to 1 for simplicity. The potential slow-roll parameters, ϵ_v and η_v, are related the Hubble slow-roll parameters, ϵ and η, by

$$\epsilon \approx \epsilon_v, \quad \eta \approx \eta_v - \epsilon_v. \tag{2.44}$$

Furthermore, the equations of motion, (2.34) and (2.35), can be reformulated as,

$$3H\dot{\phi} \approx -V_{,\phi}, \tag{2.45}$$

and,

$$H^2 \approx \frac{1}{3}V(\phi) \approx \text{const.} \tag{2.46}$$

Under the slow-roll regime, where ϵ_v and η_v are much less than 1 and spacetime is approximately de Sitter, $a(t) = e^{H_\Lambda t}$, inflation ends when the slow-roll conditions are violated,

$$\epsilon(\phi_{end}) = 1, \quad \epsilon_v(\phi_{end}) \approx 1. \tag{2.47}$$

The number of e-folds that take place during inflation can be calculated as follows:

$$\begin{aligned} N(\phi) \equiv \ln\frac{a_f}{a_i} &= \int_t^{t_{\rm end}} H\,dt \\ &= \int_\phi^{\phi_{\rm end}} \frac{H}{\dot{\phi}}\,d\phi \\ &\approx \int_{\phi_{\rm end}}^{\phi} \frac{V}{V_{,\phi}}\,d\phi \\ &= \int_{\phi_{\rm end}}^{\phi} \frac{d\phi}{\sqrt{2\epsilon}} \\ &\approx \int_{\phi_{\rm end}}^{\phi} \frac{d\phi}{\sqrt{2\epsilon_v}}. \end{aligned} \tag{2.48}$$

To solve the aforementioned horizon, flatness, and monopole problems, the total number of e-folds that occur during this period must exceed approximately 60,

$$\mathcal{N}_{\rm tot} \equiv \ln \frac{a_f}{a_i} \gtrsim 60. \tag{2.49}$$

CMB observations indicate the following constraint (Baumann 2012),

$$\int_{\phi_{\rm cmb}}^{\phi_{\rm end}} \frac{d\phi}{\sqrt{2\epsilon_v}} = \mathcal{N}_{\rm cmb} \approx 40 - 60. \tag{2.50}$$

Chapter 3

Semi-Classical Perturbations

This chapter explores the quantization of scalar perturbations during inflation. It will discuss the formation and evolution of these perturbations. Furthermore, the relevant statistical properties of these fluctuations will be derived. A crucial theoretical tool used to analyze quantum fluctuations is the analogous description of a quantum harmonic oscillator. This allows for the computation of the power spectrum of primordial perturbations. This chapter's final section will explore the ultra-slow roll theory of inflation. This possible intermediary phase during inflation would lead to a rapid increase in the generation of primordial perturbations. This framework will be used to derive the power spectrum of primordial perturbations and the occupation number of inflationary perturbations. This result will later be compared with its corpuscular counterpart.

3.1 Inflaton Perturbations

This section serves to introduce quantum fluctuations in the inflationary field. The features and evolution of these perturbations will be explored. More specifically, the phenomena of horizon exit and reentry and its impact on the growth of fluctuations will be discussed. This will be followed by a brief overview of the statistical properties used to analyze primordial perturbations, such as the power spectrum and spectral index. The connection between these values and inflationary dynamics will also be reported.

3.1.1 Primordial Perturbations

Zero-point fluctuations in the inflaton field arise due to the Heisenberg uncertainty principle and induce fluctuations in all light fields, giving way to inflaton and metric perturbations. These perturbations can also be interpreted as thermal fluctuation in de Sitter space, analogous to Hawking Radiation for a black hole. The amplitude

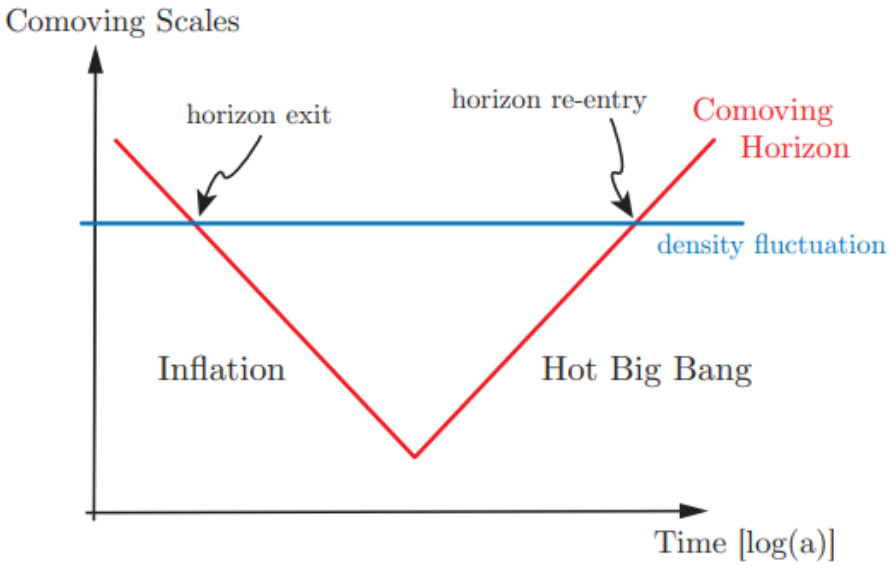

Figure 3.1: This figure depicts the time evolution of primordial density perturbations in blue and the comoving horizon in red. The scale of density fluctuations, k, is constant while the comoving horizon, $(aH)^{-1}$, shrinks during inflation and grows after inflation. Therefore, the initially subhorizon fluctuation becomes superhorizon during inflation and reenters the horizon at some point after inflation. Outside the horizon, causality is lost, and the perturbations freeze until reentry (Baumann 2012).

of these fluctuations scale with the Hubble parameter, H, which is inversely proportional to the de Sitter horizon. Quantum mechanics dictates that these fluctuations are created on all length scales and thus can be characterized by a spectrum of wavenumbers, k. The scale of these perturbations can be broken down into two cosmologically distinct categories: subhorizon scales, $k \gg aH$, and superhorizon scale, $k < aH$. While k is constant for any given perturbation, the comoving Hubble radius shrinks during inflation; thus, all perturbations eventually become superhorizon.

The inhomogeneity induced by these fluctuations can be characterized by the intrinsic curvature of spatial hypersurfaces, which has the key feature of remaining constant outside the horizon. In other words, the amplitude of primordial perturbations is constant outside the horizon shortly after inflation. This is a very convenient property, as very little is known about the universe shortly after inflation. Following inflation, the comoving horizon will grow and eventually encompass all previously superhorizon wavemodes. The comoving curvature perturbations, R, will then resume their evolution and seed the large-scale structures and CMB anisotropies observed in the universe today. Figure 3.1 depicts this phenomenon of horizon exit and reentry.

Inflationary perturbations can be analyzed through cosmological perturbation theory. One can begin to asses these perturbations by decomposing all quantities

into a homogeneous background plus a spatially dependent perturbation,

$$X(t,\vec{x}) \equiv \overline{X}(t) + \delta X(t,\vec{x}). \tag{3.1}$$

In the early universe, these perturbations are assumed to be small, $\delta X \ll \overline{X}$. Thus, the inflaton and the metric tensor can be written as,

$$\phi(t,\vec{x}) = \overline{\phi}(t) + \delta\phi(t,\vec{x}), \tag{3.2}$$

$$g_{\mu\nu}(t,\vec{x}) \equiv \overline{g}_{\mu\nu}(t) + \delta g_{\mu\nu}(t,\vec{x}). \tag{3.3}$$

As inflationary energy dominates the stress-energy of the universe during inflation, inflaton perturbations backreact on spacetime geometry. The coupling of metric and matter perturbations is given by the perturbed Einstein equation (Baumann 2012),

$$\delta G_{\mu\nu} = 8\pi G\, \delta T_{\mu\nu}. \tag{3.4}$$

3.1.2 Statistics

To avoid ambiguities due to gauge choice, cosmologists utilize gauge-invariant formulations of inflationary perturbations. For example, the gauge-invariant scalar comoving curvature perturbation can be written as,

$$R \equiv \Psi - \frac{H}{\overline{\rho}+\overline{p}}\,\delta q, \tag{3.5}$$

where, Ψ is a spatially flat hypersurface and δq is the momentum density, which can be defined as $(\delta q)_{,i} \equiv (\overline{\rho}+\overline{p})v_i$. R is a measure of the spatial curvature of comoving hypersurfaces, and it can be used to calculate the primordial power spectrum of scalar perturbations,

$$\langle R_{\vec{k}} R_{\vec{k}'}\rangle = (2\pi)^3\delta(\vec{k}+\vec{k}')P_R(k). \tag{3.6}$$

The brackets denote an ensemble average of fluctuations, and $P_R(k)$ is the power spectrum of perturbations. The dimensionless total variance of scalar perturbations can be written as,

$$\Delta_s^2 \equiv \Delta_R^2 = \frac{k^3}{2\pi^2}P_R(k). \tag{3.7}$$

One can now define the scalar spectral index as,

$$n_s - 1 \equiv \frac{d\ln\Delta_s^2}{d\ln k}, \tag{3.8}$$

and the running of the spectral index as,

$$\alpha_s \equiv \frac{dn_s}{d\ln k}. \tag{3.9}$$

These quantities can be utilized to define a power law approximation for the power spectrum,

$$\Delta_s^2(k) = A_s(k_*)\left(\frac{k}{k_*}\right)^{n_s(k_*)-1+\frac{1}{2}\alpha_s(k_*)\ln(k/k_*)}, \tag{3.10}$$

where k_* denotes an arbitrary reference scale. An analogous analysis can be made for tensor perturbations, $\Delta_t^2(k)$. The amplitude of scalar perturbations, measured as $\Delta_s^2(k) \approx 10^{-9}$, is often used to normalize the value of tensor fluctuations. A key observational probe of inflationary dynamics is the tensor-to-scalar ratio,

$$r \equiv \frac{\Delta_t^2(k)}{\Delta_s^2(k)}. \tag{3.11}$$

This ratio can be related to the evolution of the inflaton with respect to the number of e-folds by,

$$r = \frac{8}{M_{\rm pl}^2}\left(\frac{d\phi}{d\mathcal{N}}\right)^2, \tag{3.12}$$

and since the tensor fluctuations are proportional to the inflaton potential, this ratio is a direct measure of the inflationary energy scale (Baumann 2012),

$$V^{1/4} \sim \left(\frac{r}{0.01}\right)^{1/4} 10^{16}\,\text{GeV}. \tag{3.13}$$

3.2 Quantizing Primordial Perturbations

According to the semi-classical inflationary theory, inflaton perturbations must be consistent with the Heisenberg picture in order to be analyzed. Thus, they must be quantized. In curved spacetime, a harmonic oscillator can describe the inflaton field. Therefore, this section will begin by illustrating the quantum mechanics of a harmonic oscillator. This description will then be applied to inflationary dynamics to compute the power spectrum of primordial perturbations.

3.2.1 Quantum Harmonic Oscillator

Harmonic oscillators with time-dependent frequencies can describe free fields in curved spacetime. This description can be used to gather the dynamics of primordial perturbations. Therefore, understanding the quantum mechanics of a harmonic oscillator is crucial to quantifying the number of inflationary perturbations. One can begin this analysis with the classical action of a harmonic oscillator with a time-dependent frequency,

$$S = \int dt\left(\frac{1}{2}\dot{x}^2 - \frac{1}{2}\omega^2(t)x^2\right) \equiv \int dt\mathcal{L}, \tag{3.14}$$

where ω is the time-dependent frequency of the harmonic oscillator, x is the deviation of the particle's position from equilibrium, $x = 0$, and $\mathcal{L}$ is the Lagrangian. The variation of this action leads one to the following classical equation of motion,

$$\ddot{x} + \omega^2(t)x = 0. \tag{3.15}$$

The system can be canonically quantized by promoting the classical variables x and p to quantum operators $\hat{x}$ and $\hat{p}$ which satisfy,

$$[\hat{x}, \hat{p}] = i\hbar, \tag{3.16}$$

where p, the conjugate momentum, is defined as,

$$p = \frac{\partial \mathcal{L}}{\partial \dot{x}} = \dot{x}. \tag{3.17}$$

and the canonical commutator can be defined as,

$$[\hat{x}, \hat{p}] \equiv \hat{x}\hat{p} - \hat{p}\hat{x}. \tag{3.18}$$

The equation of motion implies that canonical commutation relation holds at all times if it is imposed at some initial time,

$$[x(t), \dot{x}(t)] = i\hbar. \tag{3.19}$$

Furthermore, $\hat{x}$ can be written in terms of the creation, $\hat{a}^\dagger$, and annihilation operators, $\hat{a}$,

$$\hat{x} = v(t)\hat{a} + v^*(t)\hat{a}^\dagger, \tag{3.20}$$

where the mode function, $v(t)$, satisfies the classical equation of motion,

$$\ddot{v} + \omega^2(t)v = 0, \tag{3.21}$$

and the commutator becomes,

$$\langle v, v \rangle \left[\hat{a}, \hat{a}^\dagger\right] = 1. \tag{3.22}$$

The scalar product for solutions $v(t)$ and $\omega(t)$ can be defined by,

$$\langle v, w \rangle \equiv \frac{i}{\hbar}\left(v^*\partial_t w - (\partial_t v^*)w\right). \tag{3.23}$$

This scalar product is conserved in time; it ensures that the mode functions are orthonormal and that the Wronskian condition, indicating the linear independence of solutions, is satisfied. Both of these conditions are needed to quantize the field. A properly normalized mode function satisfies $\langle v, v \rangle \equiv 1$. One can now recover the standard equation for raising and lowering operators of a harmonic oscillator,

$$\left[\hat{a}, \hat{a}^\dagger\right] = 1. \tag{3.24}$$

Thus, the creation and annihilation operators can be written as,

$$\hat{a} = \langle v, \hat{x} \rangle, \tag{165}$$

$$\hat{a}^\dagger = -\langle v^*, \hat{x} \rangle, \tag{3.25}$$

and the vacuum state can be defined as,

$$\hat{a}|0\rangle = 0. \tag{3.26}$$

Excitations of the system are produced by application of the creation operator,

$$|n\rangle \equiv \frac{1}{\sqrt{n!}} \left(\hat{a}^\dagger\right)^n |0\rangle. \tag{3.27}$$

It is evident that any change in $v(t)$ that leaves $x(t)$ unchanged will lead to a change in the creation operator and, thus, a change in the definition of the vacuum. Therefore, there is no unique choice of the mode function for a simple harmonic oscillator with a time-dependent frequency. It is convenient to consider a harmonic oscillator of constant frequency in which the preferred mode function is such that the vacuum state is the ground state of the Hamiltonian. The Hamiltonian can be written as,

$$\begin{aligned} \hat{H} &= \frac{1}{2}\hat{p}^2 + \frac{1}{2}\omega^2\hat{x}^2 \\ &= \frac{1}{2}\left[\left(\dot{v}^2 + \omega^2 v^2\right)\hat{a}\hat{a} + \left(\dot{v}^2 + \omega^2 v^2\right)^* \hat{a}^\dagger\hat{a}^\dagger \right. \\ &\quad \left. + \left(|\dot{v}|^2 + \omega^2|v|^2\right)\left(\hat{a}\hat{a}^\dagger + \hat{a}^\dagger\hat{a}\right)\right]. \end{aligned} \tag{3.28}$$

Therefore, the action of the Hamiltonian operator on the vacuum state is,

$$\hat{H}|0\rangle = \frac{1}{2}\left(\dot{v}^2 + \omega^2 v^2\right)^* \hat{a}^\dagger\hat{a}^\dagger|0\rangle + \frac{1}{2}\left(|\dot{v}|^2 + \omega^2|v|^2\right)|0\rangle. \tag{3.29}$$

The first term vanishes as $|0\rangle$ must be an eigenstate of the Hamiltonian. Thus, the mode function must satisfy the two following conditions,

$$\dot{v} = \pm i\omega v, \tag{3.30}$$

$$\langle v, v \rangle = \mp\frac{2\omega}{\hbar}|v|^2. \tag{3.31}$$

The positive-frequency solution for a normalized mode function, i.e. $\langle v, v \rangle = 1$, is,

$$v(t) = \sqrt{\frac{\hbar}{2\omega}} e^{-i\omega t}. \tag{3.32}$$

Thus, the Hamiltonian becomes,

$$\hat{H} = \hbar\omega\left(\hat{N} + \frac{1}{2}\right), \tag{3.33}$$

where $\hat{N} = \hat{a}^\dagger \hat{a}$ is the number operator, and the vacuum is the minimum energy state of $\hbar\omega/2$.

The mean square expectation value of the position operator $\hat{x}$ in the ground state is given by,

$$\begin{aligned}\langle|\hat{x}|^2\rangle &\equiv \langle 0|\hat{x}^\dagger \hat{x}|0\rangle \\ &= \langle 0|(v^*\hat{a}^\dagger + v\hat{a})(v\hat{a} + v^*\hat{a}^\dagger)|0\rangle \\ &= |v(\omega,t)|^2\langle 0|\hat{a}\hat{a}^\dagger|0\rangle \\ &= |v(\omega,t)|^2\langle 0|[\hat{a},\hat{a}^\dagger]|0\rangle \\ &= |v(\omega,t)|^2. \end{aligned} \tag{3.34}$$

Therefore, the zero-point fluctuations of the position in the vacuum state are given by the square of the mode function and thus can be written as,

$$\langle|\hat{x}|^2\rangle = |v(\omega,t)|^2 = \frac{\hbar}{2\omega}. \tag{3.35}$$

The fluctuation spectrum from inflation can now be computed if the mode equation for the scalar mode of cosmological perturbations is known (Baumann 2012).

3.2.2 Primordial Power Spectrum

Now that the dynamics of a quantum harmonic oscillator have been established, this formalism can be applied to inflationary perturbations. One can begin by considering the action of a single-field slow-roll inflationary model,

$$S = \frac{1}{2}\int d^4x\sqrt{-g}\left[R - (\nabla\phi)^2 - 2V(\phi)\right], \tag{3.36}$$

where ϕ is the inflation field, $V(\phi)$ is the inflationary potential and g is the metric tensor. The above action is defined in units where $M_{pl}^{-2} \equiv 8\pi G = 1$. The action can be expanded to the second order in terms of R,

$$S_{(2)} = \frac{1}{2}\int d^4x\, a^3 \frac{\dot{\phi}^2}{H^2}\left[\dot{R}^2 - a^{-2}(\partial_i R)^2\right]. \tag{3.37}$$

For a canonically normalized scalar, the action is found by transitioning to a conformal time, τ, and defining the Mukhanov variables, $u \equiv zR$, with $z^2 \equiv a^2\dot{\phi}^2/H^2$,

$$S_{(2)} = \frac{1}{2}\int d\tau d^3x\left[(u')^2 + (\partial_i u)^2 + \frac{z''}{z}u^2\right], \tag{3.38}$$

where commas denote derivatives with respect to conformal time. The field, u, can be Fourier expanded,

$$u(\tau,\vec{x}) = \int \frac{d^3k}{(2\pi)^3} v_{\vec{k}}(\tau)e^{i\vec{k}\cdot\vec{x}}, \tag{3.39}$$

where the mode functions are the Fourier components of the Mukhanov variable for a classical $u(\tau, \vec{x})$. The Mukhanov equation can be written as,

$$v_k'' + \left(k^2 - \frac{z''}{z}\right) v_k = 0, \tag{3.40}$$

where the vector notation on the subscript of k was dropped as this equation depends only on the magnitude of k. Additionally, it is difficult to find a general solution to (3.40) as z depends on the background dynamics; a given inflationary solution can be solved numerically. To quantize this system the field, u, and its conjugate momentum, u', can be promoted to quantum operators,

$$u \to \hat{u} = \int \frac{d^3\vec{k}}{(2\pi)^3} \left(v_k(\tau)\hat{a}_{\vec{k}} e^{i\vec{k}\cdot\vec{x}} + v_k^*(\tau)\hat{a}_{\vec{k}}^\dagger e^{-i\vec{k}\cdot\vec{x}}\right). \tag{3.41}$$

Furthermore, the Fourier components, $u_{\vec{k}}$, can be quantized as,

$$u_{\vec{k}} \to \hat{u}_{\vec{k}} = v_k(\tau)\hat{a}_{\vec{k}} + v_{-k}^*(\tau)\hat{a}_{-\vec{k}}^\dagger. \tag{3.42}$$

The creation and annihilation operators satisfy the canonical commutation relation,

$$[\hat{a}_{\vec{k}}, \hat{a}_{\vec{k}}^\dagger] = (2\pi)^3\delta(\vec{k} - \vec{k}'), \tag{3.43}$$

if and only if the mode functions can be normalized as,

$$\langle v_k, v_k\rangle \equiv \frac{i}{\hbar}\left(v_k^* v_k' - v_k^{*\prime} v_k\right). \tag{3.44}$$

This is the Klein-Gordon scalar product for the modes, which is conserved in conformal time, τ. It ensures orthonormality and that the Wronskian condition is satisfied. The proper normalization condition for the mode functions is given by $\langle v_k, v_k\rangle = 1$. One can now define a vacuum state for the fluctuations, $\hat{a}_{\vec{k}}|0\rangle = 0$, and impose boundary conditions on the mode function. A common choice is the Minkowski vacuum of a comoving observer in the far past, thus $\tau \to -\infty$, or equivalently, $k \gg aH$. The Mukhanov equation then becomes the equation for a simple harmonic oscillator with a time-independent frequency,

$$v_k'' + k^2 v_k = 0. \tag{3.45}$$

If the vacuum is the minimum energy state, a unique solution for the mode function can be found; thus, the following initial condition should be imposed,

$$\lim_{\tau\to-\infty} v_k = \frac{e^{-ik\tau}}{\sqrt{2k}}. \tag{3.46}$$

In de Sitter space, $\epsilon \Rightarrow 0$, and,

$$\frac{z''}{z} = \frac{a''}{a} = \frac{2}{\tau^2}. \tag{3.47}$$

Therefore, the Mukhanov equation becomes,

$$v_k'' + \left(k^2 - \frac{2}{\tau^2}\right) v_k = 0, \tag{3.48}$$

and is solved by,

$$v_k = \alpha \frac{e^{-ik\tau}}{\sqrt{2k}} \left(1 - \frac{i}{k\tau}\right) + \beta \frac{e^{ik\tau}}{\sqrt{2k}} \left(1 + \frac{i}{k\tau}\right), \tag{3.49}$$

where α and β account for the nonuniqueness of the mode functions. Considering the normalization of the mode function and the subhorizon limit, α and β can be fixed to 1 and 0, respectively. This defines the Bunch-Davies mode functions,

$$v_k = \frac{e^{-ik\tau}}{\sqrt{2k}} \left(1 - \frac{i}{k\tau}\right). \tag{3.50}$$

The power spectrum of curvature perturbations in a quasi-de Sitter universe can now be computed. One can begin by considering the field, $\hat{\psi}_{\vec{k}} \equiv \hat{u}_{\vec{k}}/a$; its power spectrum is,

$$\begin{aligned} \langle \hat{\psi}_{\vec{k}}(\tau) \hat{\psi}_{\vec{k}'}(\tau) \rangle &= (2\pi)^3 \delta(\vec{k} + \vec{k}') \frac{|u_k(\tau)|^2}{a^2} \\ &= (2\pi)^3 \delta(\vec{k} + \vec{k}') \frac{H^2}{2k^3} \left(1 + k^2\tau^2\right). \end{aligned} \tag{3.51}$$

On super horizon scales, $|k\tau| \ll 1$, the $k^2\tau^2$ term is negligible. The power spectrum of curvature perturbations at horizon crossing, $a(t_*)H(t_*) = k$, can be computed considering, $R = \psi H/\dot{\phi}$.

$$\langle R_{\vec{k}}(t) R_{\vec{k}'}(t) \rangle = (2\pi)^3 \delta(\vec{k} + \vec{k}') \frac{H_*^2}{2k^3} \frac{H_*^2}{\dot{\phi}_*^2} \tag{3.52}$$

where the astrix indicates that the quantity should be evaluated at horizon crossing. The dimensionless power spectrum, $\Delta_R^2(k)$ is defined by,

$$\langle R_{\vec{k}} R_{\vec{k}'} \rangle = (2\pi)^3 \delta(\vec{k} + \vec{k}') P_R(k), \tag{3.53}$$

$$\Delta_R^2(k) \equiv \frac{k^3}{2\pi^2} P_R(k) \tag{3.54}$$

Thus,

$$\Delta_R^2(k) = \frac{H_*^2}{(2\pi)^2} \frac{H_*^2}{\dot{\phi}_*^2} \tag{3.55}$$

As R approaches a constant on superhorizon scales, computing its value at horizon crossing is sufficient to determine the spectrum of a given fluctuation until it reenters the horizon. However, it should be noted that the above result holds during slow-roll inflation; for non-slow-roll inflation, the background evolution must be more carefully tracked; this can be done by numerically integrating the Mukhanov equation (Baumann 2012).

3.3 Ultra-Slow Roll Inflation

This section will focus on a theorized period of inflation known as ultra-slow roll inflation, in which the power spectrum experiences exponential growth. The governing dynamics of this phase will be described, and the power spectrum of curvature perturbations generated during this phase will be reported. Subsequently, the occupation number of inflationary perturbations will be derived, and its exponential dependence on the number of e-foldings will be discussed.

3.3.1 Ultra-Slow Roll Phase

Some semi-classical inflationary models predict a possible intermediary phase during inflation known as the ultra-slow roll (USR) phase. This phase has gained favor in inflationary theory because it would increase the production of primordial black holes; however, it is not universally accepted. Inflationary theory predicts that the inflaton starts at large field values and inflation ends when the field reaches an absolute minimum. USR theory predicts that before the end of inflation, the potential approaches a stationary inflection point with a local minimum followed by a local maximum. As the inflaton approaches this point, its velocity approaches zero. However, it has just enough inertia to overcome this barrier; this is the USR phase. It lasts approximately 2.45 e-folds and is characterized by a slow roll parameter $\eta > 3$. Wave modes that exit the horizon during this phase are subject to an exponential enhancement of the power spectrum. During the USR phase, the evolution of the perturbations, as described by a harmonic oscillator, is driven by the friction term, which changes signs during this phase and leads to the enhancement of the power spectrum. This exponential enhancement can be gathered from the following equation of motion,

$$\frac{d^2h}{d\mathcal{N}^2} + 3\frac{dh}{d\mathcal{N}} - \frac{1}{2}\left(\frac{dh}{d\mathcal{N}}\right)^3 + \left(3 - \frac{1}{2}\left(\frac{dh}{d\mathcal{N}}\right)^2\right)\frac{d\log U}{dh} = 0, \tag{3.56}$$

where h is the canonically normalized inflaton field, ϕ, satisfying $h(\phi = 0) = 0$, U is the potential of the canonically normalized field, and $\mathcal{N}$ is the number of e-folding. Furthermore, the power spectrum is approximated by,

$$P_R(k) = \frac{H^2}{8\pi^2\epsilon}\left(\frac{k}{aH}\right)^{-4\epsilon+2\eta} = A_s\left(\frac{k}{aH}\right)^{n_s-1}. \tag{3.57}$$

When the inflaton approaches the inflection point, and its velocity suddenly decreases, the power spectrum increases by $P_R(k) \propto 1/\epsilon$, where $\epsilon \propto (dh/d\mathcal{N})^2$. However, the above approximation is not sufficient to account for the power spectrum

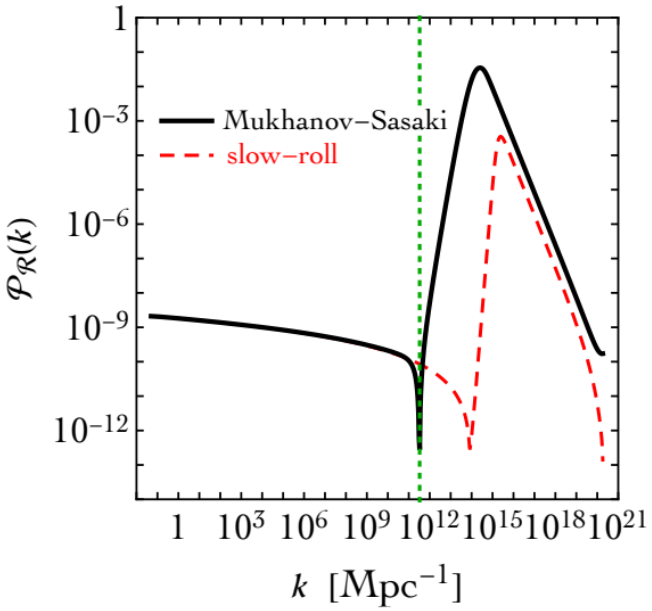

Figure 3.2: This figure reports the power spectrum of comoving curvature perturbations as a function of the comoving scale k. The result obtained by numerically solving the Mukhanov-Sasaki equation is shown by the solid black curve, while the approximate power spectrum given by (3.57) is represented by the dashed red curve. The dotted green line marks the value of k at which the spectrum has a pronounced dip (Ballesteros et al. 2020a).

at small scales during the USR phase; for this, one needs the Mukhanov-Sasaki equation in Fourier space,

$$\frac{d^2 u_{\vec{k}}}{d\mathcal{N}^2} + (1-\epsilon)\frac{du_{\vec{k}}}{d\mathcal{N}} + \left[\frac{k^2}{a^2H^2} + (1+\epsilon-\eta)(\eta-2) - \frac{d}{d\mathcal{N}}(\epsilon-\eta)\right] u_{\vec{k}} = 0, \qquad (3.58)$$

where the perturbation of the inflation field in Fourier space, $u_{\vec{k}}$, is related to the comoving curvature perturbation, R, by $R = -u/z$, with $z = a(dh/d\mathcal{N})$. Imposing Bunch-Davies initial condition, the power spectrum becomes,

$$P_R(k) = \frac{k^3}{2\pi^2}\left|\frac{u_{\vec{k}}}{z}\right|^2_{k\ll aH}, \qquad (3.59)$$

where the contribution of each mode, k, is constant as it is evaluated on superhorizon scales. The Mukhanov-Saski equation, (3.58), can be numerically evaluated and compared to the slow-roll approximation of the power spectrum given by (3.57) as depicted in Figure 3.2. At small k, the approximate solution sufficiently reproduces the value of the power spectrum. However, at large k, the power spectrum experiences a sudden dip followed by rapid power-law growth. The power spectrum peaks at $k \approx 10^{14}\text{Mpc}^{-1}$ with an amplitude of $A_s \approx 10^{-1}$. The difference between the approximate and numerical solution in this region is a couple of orders of magnitude and, therefore, is relevant in quantifying the number of primordial perturbations.

Additionally, from the inflaton's equation of motion, (3.56), one can find,

$$\eta = 3 + (3 - \epsilon)\frac{d\log U}{dh}\left(\frac{dh}{d\mathcal{N}}\right)^{-1} \tag{3.60}$$

which must be greater than three during the USR phase. In other words, the second term in this equation becomes positive. The impact of this condition on the power spectrum is evident by the equation for the comoving curvature perturbation in Fourier space,

$$\frac{d^2R_{\vec{k}}}{d\mathcal{N}^2} + (3 + \epsilon - 2\eta)\frac{dR_{\vec{k}}}{d\mathcal{N}} + \frac{k^2}{a^2H^2}R_{\vec{k}} = 0. \tag{3.61}$$

This is analogous to the equation for a damped harmonic oscillator. After a wave mode crosses the horizon, it freezes exponentially fast to a constant value. This is because if $2\eta - \epsilon > 3$ holds during the subsequent evolution of the inflaton, the friction term in the above equation will become negative, leading to an exponential growth of the wave mode. This can be shown by finding a solution to the above equation considering,

$$\Theta \equiv 3 + \epsilon - 2\eta, \quad \epsilon_k^2 \equiv \frac{k^2}{a^2H^2}. \tag{3.62}$$

Additionally, one can define $\mathcal{N}_{in}$ and $\mathcal{N}_{end}$ as the e-folds at the start and end of the negative friction phase and consider the following boundary conditions,

$$R_{\vec{k}}(\mathcal{N}_{\rm in}) = R_0, \quad \frac{dR_{\vec{k}}}{d\mathcal{N}}(\mathcal{N}_{in}) = 0. \tag{3.63}$$

This indicates that the mode froze before the negative friction phase. One can now find a solution for (3.61),

$$\begin{aligned}\tilde{R}_{\vec{k}}(\mathcal{N}_e) = \frac{R_0 e^{-\Theta(\mathcal{N}_e - \mathcal{N}_{\rm in})/2}}{\sqrt{\Theta^2 - 4\epsilon_k^2}}\Bigg\{&\sqrt{\Theta^2 - 4\epsilon_k^2}\cosh\left(\frac{\mathcal{N} - \mathcal{N}_{\rm in}}{2}\sqrt{\Theta^2 - 4\epsilon_k^2}\right)\\ &+ \Theta\sinh\left(\frac{\mathcal{N} - \mathcal{N}_{\rm in}}{2}\sqrt{\Theta^2 - 4\epsilon_k^2}\right)\Bigg\}.\end{aligned} \tag{3.64}$$

The first term is, $\approx e^{-\Theta\mathcal{N}/2}$ and leads to exponential growth if Θ is negative. The term within the brackets represents a non-oscillating super-position of $e^{\pm\sqrt{\Theta^2-4\epsilon_k^2}\mathcal{N}/2}$ if $\Theta^2 - 4\epsilon_k^2 > 0$. It is now evident that the USR phase can exponentially enhance the power spectrum (Ballesteros et al. 2020a).

3.3.2 Occupation Number of Perturbations

One can find that the number of inflationary perturbations also grows exponentially. To explicitly define the exponential growth of the occupation number in the semi-classical inflationary model, one needs to write the time-dependent occupation

number in terms of the expectation value of the time-dependent particle number operator, $a^{\dagger}_{\vec{k}}(\tau)a_{\vec{k}}(\tau)$, in its original vacuum state. One can begin this computation by considering a perturbation, $u(\tau,\vec{x})$, that satisfies the following equation of motion,

$$\left(\frac{d^2}{d\tau^2}-\Delta-\frac{1}{z}\frac{d^2z}{d\tau^2}\right)u(\tau,\vec{x})=0. \tag{3.65}$$

The following notation $' \equiv d/d\tau$ and $(\partial u)^2=(\partial_i u)(\partial_i u)$ will be used for simplicity. This equation of motion can be derived from the following action,

$$S_2=\frac{1}{2}\int d\tau d^3\vec{x}\left[\left(u'-\frac{z'}{z}u\right)^2-(\partial u)^2\right]. \tag{3.66}$$

The relation between the above two equations is made more explicit with the identity,

$$(u')^2+\frac{z''}{z}u^2=\left(u'-\frac{z'}{z}u\right)^2+\left(\frac{z'}{z}u^2\right)'. \tag{3.67}$$

The corresponding Hamiltonian can be written as,

$$H(\tau)=\frac{1}{2}\int d^3\vec{x}\left(p^2+(\partial u)^2+\frac{2z'}{z}pu\right), \tag{3.68}$$

where, the conjugate momentum can be defined as $p=\delta S_2/\delta u'=u'-u(z'/z)$. One can now promote $u(\tau,\vec{x})$ and $p(\tau,\vec{x})$ to quantum operators, $\hat{u}(\tau,\vec{x})$ and $\hat{p}(\tau,\vec{x})$ that in real space satisfy the following commutation relation,

$$[\hat{u}(\tau,\vec{x}),\hat{p}(\tau,\vec{x}')]=i\delta^{(3)}(\vec{x}-\vec{x}'). \tag{3.69}$$

Moving to Fourier space, the quantized Hamiltonian can be written as

$$\begin{aligned}\hat{H}(\tau)=\frac{1}{2}\int d^3\vec{k}\Big[&\hat{p}(\tau,\vec{k})\hat{p}^{\dagger}(\tau,\vec{k})+k^2\hat{u}(\tau,\vec{k})\hat{u}^{\dagger}(\tau,\vec{k})\\&+\frac{z'}{z}\left[\hat{p}(\tau,\vec{k})\hat{u}^{\dagger}(\tau,\vec{k})+\hat{u}(\tau,\vec{k})\hat{p}^{\dagger}(\tau,\vec{k})\right]\Big],\end{aligned} \tag{3.70}$$

where $\hat{u}(\tau,\vec{k})$ and $\hat{p}(\tau,\vec{k})$ satisfy the following commutation relations,

$$[\hat{u}(\tau,\vec{k}),\hat{p}(\tau,\vec{k}')]=i\delta^{(3)}(\vec{k}+\vec{k}'), \tag{3.71}$$

$$[\hat{u}(\tau,\vec{k}),\hat{p}^{\dagger}(\tau,\vec{k}')]=i\delta^{(3)}(\vec{k}-\vec{k}'). \tag{3.72}$$

To evaluate the evolution of this quantum system, it is useful to define the creation and annihilation operators,

$$a^{\dagger}_{\vec{k}}(\tau)=\sqrt{\frac{k}{2}}\hat{u}^{\dagger}(\tau,\vec{k})-\frac{i}{\sqrt{2k}}\hat{p}^{\dagger}(\tau,\vec{k})=\sqrt{\frac{k}{2}}\hat{u}(\tau,-\vec{k})-\frac{i}{\sqrt{2k}}\hat{p}(\tau,-\vec{k}), \tag{3.73}$$

$$a_{\vec{k}}(\tau)=\sqrt{\frac{k}{2}}\hat{u}(\tau,\vec{k})+\frac{i}{\sqrt{2k}}\hat{p}(\tau,\vec{k}). \tag{3.74}$$

The evolution of $\hat{u}(\tau, \vec{x})$ and $\hat{p}(\tau, \vec{x})$ can be written in terms of these ladder operators,

$$\hat{u}(\tau, \vec{k}) = \frac{1}{\sqrt{2k}} \left[a_{\vec{k}}(\tau) + a^{\dagger}_{-\vec{k}}(\tau) \right], \tag{3.75}$$

$$\hat{p}(\tau, \vec{k}) = -i\sqrt{\frac{k}{2}} \left[a_{\vec{k}}(\tau) - a^{\dagger}_{-\vec{k}}(\tau) \right], \tag{3.76}$$

where the ladder operators satisfy the following commutation relation,

$$[a_{\vec{k}}(\tau), a^{\dagger}_{\vec{k}'}(\tau)] = \delta^{(3)}(\vec{k} - \vec{k}'). \tag{3.77}$$

The Hamiltonian can now be written as,

$$\begin{aligned} \hat{H}(\tau) = \frac{1}{2} \int d^3\vec{k} \Big[k \Big(a_{\vec{k}}(\tau) a^{\dagger}_{\vec{k}}(\tau) + a^{\dagger}_{-\vec{k}}(\tau) a_{-\vec{k}}(\tau) \Big) \\ + \frac{i}{z} \frac{dz}{d\tau} \Big(a^{\dagger}_{-\vec{k}}(\tau) a^{\dagger}_{\vec{k}}(\tau) - a_{\vec{k}}(\tau) a_{-\vec{k}}(\tau) \Big) \Big]. \end{aligned} \tag{3.78}$$

Additionally, the Heisenberg equations of motion take a matrix form,

$$\frac{d}{d\tau} \begin{pmatrix} a_{\vec{k}}(\tau) \\ a^{\dagger}_{-\vec{k}}(\tau) \end{pmatrix} = \begin{pmatrix} -ik & z'/z \\ z'/z & ik \end{pmatrix} \begin{pmatrix} a_{\vec{k}}(\tau) \\ a^{\dagger}_{-\vec{k}}(\tau) \end{pmatrix}. \tag{3.79}$$

It can be noted from this equation that in curved spacetime, the off-diagonal terms in this matrix are responsible for particle creation. Next, one can utilize the following Bogoliubov transformation,

$$a_{\vec{k}}(\tau) = y_{\vec{k}}(\tau) a_{\vec{k}}(\tau_*) + w_{\vec{k}}(\tau) a^{\dagger}_{-\vec{k}}(\tau_*), \tag{3.80}$$

$$a^{\dagger}_{-\vec{k}}(\tau) = y^*_{\vec{k}}(\tau) a^{\dagger}_{-\vec{k}}(\tau_*) + w^*_{\vec{k}}(\tau) a_{\vec{k}}(\tau_*), \tag{3.81}$$

where τ_* is some initial conformal time. The commutation relations of these operators indicate the following condition: $|y_{\vec{k}}(\tau)|^2 - |w_{\vec{k}}(\tau)|^2 = 1$. Equations (3.75) and (3.76) now take the form of,

$$\hat{u}(\tau, \vec{k}) = u_{\vec{k}}(\tau) a_{\vec{k}}(\tau_*) + u^*_{\vec{k}}(\tau) a^{\dagger}_{-\vec{k}}(\tau_*), \tag{3.82}$$

$$\hat{p}(\tau, \vec{k}) = -i \left(p_{\vec{k}}(\tau) a_{\vec{k}}(\tau_*) - p^*_{\vec{k}}(\tau) a^{\dagger}_{-\vec{k}}(\tau_*) \right), \tag{3.83}$$

where $u_{\vec{k}}(\tau)$ and $p_{\vec{k}}(\tau)$ are defined as,

$$u_k(\tau) \equiv \frac{1}{\sqrt{2k}} \left(y_{\vec{k}}(\tau) + w^*_k(\tau) \right), \tag{3.84}$$

$$p_k(\tau) \equiv \sqrt{\frac{k}{2}} \left(y_{\vec{k}}(\tau) - w^*_k(\tau) \right). \tag{3.85}$$

It is now evident that $\hat{u}(\tau, \vec{x})$ and $\hat{p}(\tau, \vec{x})$ satisfy the equation of motion, (3.65),

$$\frac{d^2 u_k}{d\tau^2} + \left(k^2 - \frac{1}{z} \frac{d^2 z}{d\tau^2} \right) u_k = 0, \quad \text{with } u_k(\tau_*) = \frac{1}{\sqrt{2k}}, \tag{3.86}$$

$$p_k(\tau) = i\left(\frac{du_k}{d\tau} - \frac{1}{z}\frac{dz}{d\tau}u_k\right), \quad \text{with} \quad p_k(\tau_*) = \sqrt{\frac{k}{2}}. \tag{3.87}$$

Furthermore, the Wronskian condition, indicating the linear independence of solutions, can be realized from the condition, $|y_{\vec{k}}(\tau)|^2 - |w_{\vec{k}}(\tau)|^2 = 1$, as well as, equations (3.84) and (3.85),

$$p_k(\tau)u_k^*(\tau) + p_k^*(\tau)u_k(\tau) = 1 \Rightarrow i\left(\frac{du_k(\tau)}{d\tau}u_k^*(\tau) - \frac{du_k^*(\tau)}{d\tau}u_k(\tau)\right) = 1. \tag{3.88}$$

One can now proceed with computing the occupation number of inflaton perturbations. The first step is to solve the system of equations given by (3.86) and (3.87). Then the evolution of the ladder operators defined in equations (3.80) and (3.81) can be calculated by inverting equations (3.84) and (3.85). Note that in this computation, the vector notation of k is dropped as the mode functions depend only on the modulus of k. The initial conditions of u_k and p_k can be gathered from the ladder operators, (3.80) and (3.81). The initial condition of τ_* follows from the standard inflationary assumption that the system starts in the vacuum state, $|0\rangle$, defined as, $a_{\vec{k}}(\tau_*)|0\rangle = 0$. Lastly, the time-dependent particle number operator can be defined as $a_k^\dagger(\tau)a_k(\tau)$. The time-dependent occupation number, $N_k(\tau)$, defined for each mode k, is given by the expectation value in the original vacuum state of the time-dependent particle number operator. Therefore,

$$\begin{aligned}
\bar{n}_{\vec{k}}(\tau) &= \langle 0|a_{\vec{k}}^\dagger(\tau)a_{\vec{k}}(\tau)|0\rangle \\
&= \langle 0|\left(y_k^*(\tau)a_{\vec{k}}^\dagger(\tau_*) + w_k^*(\tau)a_{-\vec{k}}(\tau_*)\right) \\
&\quad \left(y_k(\tau)a_{\vec{k}}(\tau_*) + w_k(\tau)a_{-\vec{k}}^\dagger(\tau_*)\right)|0\rangle \\
&= |w_k(\tau)|^2\,\delta^{(3)}(0) \equiv n_k(\tau)\delta^{(3)}(0).
\end{aligned} \tag{3.89}$$

The delta function, $\delta^{(3)}$, can be interpreted as the spatial volume in momentum space. This arises because the total number of particles is calculated rather than the particle number density, $n_k(\tau) = |w_k(\tau)|^2$. The final step is to solve equations (3.84) and (3.85) for ${w_k}^*$. This, in conjunction with the Wronskian condition, can be used to recover the occupation number density,

$$n_k(\tau) = \frac{k}{2}|u_k(\tau)|^2 + \frac{1}{2k}|p_k(\tau)|^2 - \frac{1}{2}. \tag{3.90}$$

Using this formula Ballesteros et al. 2020b computes the occupation number of perturbations during the USR phase. The equation of motion, (3.65), can be solved by,

$$u_k(\tau) = \alpha_k v_k(\tau) + \beta_k v_k^*(\tau), \tag{3.91}$$

where,

$$v_k(\tau) = \sqrt{\frac{\pi}{2}}e^{i(\nu+1/2)\pi/2}\sqrt{-\tau}H_\nu^{(1)}(-k\tau), \tag{3.92}$$

where, $H_\nu^{(1)}$ is the Hankel function of the first kind which should be computed at the horizon crossing time for the mode k, $\nu = \sqrt{9/4 - \eta(3-\eta)}$, and the complex coefficients satisfy the Wronskian condition, $|\alpha_k|^2 - |\beta_k|^2 = 1$. One can now find that the occupation number takes the form of,

$$n_k(\tau) = \frac{\pi}{8}(-k\tau)\left(|\tilde{\alpha}_k|^2 + |\tilde{\beta}_k|^2 + \left[\tilde{\alpha}_k(\tilde{\beta}_k)^* e^{i\pi(\nu+1/2)}\right] + \text{c.c.}\right), \tag{3.93}$$

where,

$$|\tilde{\alpha}_k|^2 + |\tilde{\beta}_k|^2 = -\frac{4}{\pi(-k\tau)}\left(|\tilde{\alpha}_k|^2 + |\tilde{\beta}_k|^2\right) \tag{3.94}$$

$$\times \left[\left(1+\kappa^2\right) H_\nu^{(1)} H_\nu^{(2)} + H_{\nu-1}^{(1)} H_{\nu-1}^{(2)} + \kappa\left(H_\nu^{(1)} H_{\nu-1}^{(2)} + H_\nu^{(2)} H_{\nu-1}^{(1)}\right)\right], \tag{3.95}$$

and,

$$\tilde{\alpha}_k(\tilde{\beta}_k)^* = \alpha_k(\beta_k)^*\left((1+\kappa^2) H_\nu^{(1)} H_\nu^{(1)} + H_{\nu-1}^{(1)} H_{\nu-1}^{(1)} + 2\kappa H_\nu^{(1)} H_{\nu-1}^{(1)}\right), \tag{3.96}$$

where $\kappa \equiv (3/2 - \nu - \eta)\,/\,(-k\tau)$. Furthermore, to evaluate this, one can use,

$$-k\tau = x e^{\mathcal{N}_{\text{in}} - \mathcal{N}}, \quad x \equiv \frac{k}{k_{\text{in}}} \tag{3.97}$$

where $\mathcal{N}_{in}$ marks the number of e-foldings beginning of the USR phase. It should be noted that these equations can be evaluated for various inflationary phases, but for this paper, they need only be evaluated at the USR phase. The USR phase, which spans from $\mathcal{N}_{in}$ to $\mathcal{N}_{end}$, is such that $x \ll e^{\mathcal{N}-\mathcal{N}_{\text{in}}}$, thus the occupation number takes the form of,

$$n_{x \ll e^{\mathcal{N}-\mathcal{N}_{\text{in}}}} \propto e^{(2\nu+1)\mathcal{N}}. \tag{3.98}$$

In summation, the occupation number of inflationary perturbation grows exponentially with the number of e-folding under a semi-classical inflationary model (Ballesteros et al. 2020b).

Chapter 4

Corpuscular Cosmology

This chapter will focus on a corpuscular theory of cosmology. This model was first utilized to describe black hole dynamics, and a brief explanation of this prescription will be given. This model will then be generalized to all maximally symmetric cosmological spaces. The efficacy of this generalization, its effect on the interpretation of cosmological phenomena, and its benefits over the semi-classical model will be discussed. The focus of the chapter will then turn to a corpuscular model of inflation and the generation of primordial perturbations. Under the corpuscular model, perturbations arise due to the depletion of the condensate background. The dynamics of corpuscular inflation will be explored, and the depletion rate of the background universe will be derived.

4.1 Corpuscular Theory

This section introduces corpuscular theory, in which a gravitational system can be described by a quantum condensate of gravitons characterized by a wavelength, λ, and an occupation number, N. This theory was first used to describe a black hole as a condensate at a critical point of a quantum phase transition. In this description, Hawking radiation manifests as the depletion of the condensate. Furthermore, this theory can be extended to any maximally symmetric space, setting the stage for a fully quantum cosmological model.

4.1.1 Quantum Picture of a Black Hole

Dvali and Gomez first posited the corpuscular picture to describe black holes in their 2011 paper 'Black Hole's Quantum N-Portrait.' While black holes are not the subject of this paper, it is useful to understand their original hypothesis. Dvali and Gomez aim to provide a quantum theory of gravity with a weakly coupled quantum particle with zero mass and spin-2. The self-coupling of these gravitons can be

defined as,

$$\alpha \equiv \hbar G \lambda^{-2} \quad \text{or} \quad \frac{\ell_p^2}{\lambda^2}, \tag{4.1}$$

where λ is the wavelength of the constituent gravitons and ℓ_p is the Planck length. Einstein's gravity is hypothesized as a quantum theory in which gravitons can account for all the properties of a black hole. Along these lines, any classical object can be described as a quantum state with an occupation number greater than 1, characterized by a wavelength and a frequency. A black hole can then be described as a bose-condensate of N weakly interacting soft-gravitons. The occupation number of this condensate is given by,

$$N = \frac{M r_g}{\hbar}, \tag{4.2}$$

where r_g is the gravitational radius of the black hole and M is the mass. The wavelength of the constituent quanta is given by,

$$\lambda = \sqrt{N}\ell_p, \tag{4.3}$$

and the binding potential of the condensate is given by,

$$V = \frac{\hbar}{\sqrt{N}\ell_p}. \tag{4.4}$$

Note that this equation also serves as the thermal spectrum of Hawking radiation. A key finding of this picture is its explanation of Hawking radiation as the quantum depletion of the condensate. Depletion occurs if a constituent graviton gains energy above $\hbar/\lambda$, causing it to 'leak out' of the condensate. An evaporation rate can characterize the depletion of a black hole,

$$\frac{dN}{dt} = -\frac{1}{\sqrt{N}\ell_p}, \tag{4.5}$$

with a half-life of,

$$\tau = N^{\frac{3}{2}}\ell_p. \tag{4.6}$$

Moreover, every property of the condensate can be described in terms of its occupation number. The wavelength scales with $\sqrt{N}$, the coupling strength scales with $1/N$, and the mass of the condensate also scales with $\sqrt{N}$ (Dvali and Gomez 2011). In 2012, Dvali and Gomez reformulated their theory with an addendum specifying that the condensate exists at a critical point of a quantum phase transition between a graviton-Bose-gas and a graviton-Bose-liquid. In this manner, the Bogoliubov modes that become degenerate and nearly gapless are the holographic degrees of freedom responsible for the entropy and information storage of the black hole. They explain how such a condensate adheres to a maximal packing condition. This condition ensures that the occupation number is related to the size of the condensate. It is impossible to increase the occupation number without increasing the condensate size (Dvali and Gomez 2012).

4.1.2 Generalization to Cosmological Spaces

In their 2014 paper, "Quantum compositeness of gravity: black holes, AdS, and inflation," Dvali and Gomez claimed this composite theory could be extended to other gravitational systems, such as any maximally symmetric space. This claim was further supported by discovering that the corpuscular picture recovers the AdS/CFT correspondence. This correspondence describes the phenomenon in which a Conformal Field Theory (CFT), which lacks gravity, can be defined on the boundary of an Anti-de Sitter (AdS) spacetime. In other words, a gravitational theory defined on an (n+1)-dimensional AdS space can be equivalently defined by an n-dimensional CFT. Remarkably, when the corpuscular picture is ascribed to AdS space, the occupation number of gravitons correlates to the central charge of a CFT. This implies that a quantum composite description could explain holography, hence the importance of extrapolating this black hole picture to any gravitational system. Dvali and Gomez defined their hypothesis as follows: "Gravitational systems, such as black holes, AdS, de Sitter or other cosmological spaces represent composite entities of microscopic quantum constituent gravitons of wavelength set by the characteristic classical size R (i.e., the curvature radius) of the system" (Dvali and Gomez 2014).

It was subsequently demonstrated that in the corpuscular description, the standard curved metric description of gravity can be realized in the limit where the occupation number of gravitons goes to infinity. As such, the dynamics of a point source in a classical background can be described as a quantum scattering of the point source off the constituent off-shell gravitons. This motion is recovered from the following matrix elements,

$$\langle N+1|a^\dagger|N\rangle \sim \frac{\sqrt{\hbar}}{R}\sqrt{(N+1)}, \quad \langle N|a^\dagger a|N\rangle \sim \frac{\hbar}{R^2}N\ldots \tag{4.7}$$

where $|N\rangle$ is the quantum state of the background, R is the wavelength of the gravitons, and a and $a^\dagger$ are ladder operators. If all composite gravitons remain off-shell, one can recover the classical metric, which lacks particle creation. However, if the condensate undergoes some process in which some amount of the composite gravitons is left on-shell, i.e., some gravitons can propagate, this would lead to particle creation. Thus, particle creation is no longer a vacuum process but is intrinsically tied to the scattering of the constituent gravitons that make up the background. The background becomes effectively classical only in the limit where $N \to \infty$ and particle creation appears to be a vacuum process. As the background can be assumed to be classical in this limit and has an infinite particle creation capacity, it is thus eternal. However, the issue with this argument lies in the eternal condition of the background, as in an eternal background, entanglement can not be measured at some finite time and is thus arbitrary. Outside this limit, i.e., for

a background with a finite occupation number, achieving maximum entanglement would require a number of steps of order N and could not be achieved from a single emission. In the corpuscular description, particle creation can only occur in spacetimes without a globally defined time. This is because, in such spacetimes, the composite system is in a state of quantum criticality, meaning that its gravitons have non-zero frequencies. This frequency condition allows the gravitons to scatter and produce on-shell particles. However, in static spacetimes, characterized by globally defined time, the condensate does not meet a quantum criticality condition, the gravitons have null frequencies, and the production of on-shell particles does not occur (Dvali and Gomez 2014).

4.2 Inflation and Depletion

In this section, the corpuscular description is applied to the inflationary epoch. In this description, each inflationary Hubble patch can be considered a condensate composed of inflatons and gravitons. By the nature of this condensate, the composite quanta scatter and deplete. This depletion is the driver of inflation under this purely quantum model, in contrast to the scalar field of the semi-classical model. Inflation ends once depletion is no longer energetically favorable. Therefore, the depletion rate can constrain the duration of inflation. The depleted quanta that are 'squeezed out' of the condensate during inflation constitute the primordial perturbations evidenced by the CMB. This section will explore inflationary dynamics under a corpuscular model and the depletion mechanism. Additionally, the depletion rate of the inflationary background will be derived.

4.2.1 Corpuscular Inflation

A corpuscular interpretation of inflationary cosmology can provide theorists with an alternative explanation of the driving forces behind inflation and bring forth new information about that era that is not recoverable in a semi-classical picture. The general idea put forth by Dvali and Gomez is to apply the compositeness description, particularly with a large-N approximation, to de Sitter spacetime or other inflationary universes to recover well-known predictions of inflation, such as primordial perturbations. According to this description, inflation would end when the composite background stops depleting. A unique benefit of the corpuscular picture is that the time evolution of the universe during the inflationary epoch is easier to map as the background acts as a quantum clock. Due to the process of depletion, the composite background imprints measurable effects onto observables such as the CMB. These effects accumulate throughout the entire inflationary duration. Therefore, applying this methodology can recover information about the entire history

of inflation, which would be inaccessible with a semi-classical approach (Dvali and Gomez 2014).

Under the corpuscular picture, each inflationary Hubble patch, with radius R_H, is treated as a reservoir with a finite number of quanta, a Bose-Einstein condensate. The occupation number of gravitons in each patch is given by,

$$N = \left(\frac{R_H}{\ell_p}\right)^2, \tag{4.8}$$

where ℓ_p is Planck length and can be related to Newton's constant by $\ell_p^2 = \hbar G$. Similar to the aforementioned black hole description, the condensate is near a point of quantum criticality and thus undergoes depletion. Throughout the inflationary era, the occupation number of the background condensate decreased, and the inflationary mechanism was the emptying of this reservoir. However, the inflationary condensate background differs from the black hole case as it consists of two species of quanta: inflatons and gravitons. This difference is crucial as the inflaton background, a Bose gas with occupation number $N_\phi \gg N$, assists in the depletion. This assistance is simply because if the number of different species of quanta increases, the number of channels by which quanta can scatter and deplete increases as well.

A key finding is that the occupation numbers of each species can be related to inflationary dynamics through the slow-roll parameter, ϵ

$$\frac{N}{N_\phi} = \sqrt{\epsilon}, \tag{4.9}$$

where,

$$\epsilon \equiv \left(\frac{V'}{V\ell_p}\right)^2 \hbar, \tag{4.10}$$

again, the comma denotes a derivative with respect to ϕ. This indicates that the speed at which the inflaton rolls down its nearly flat potential is inversely proportional to N_ϕ/N. In other words, the greater the duration of inflation, the larger the inflaton to graviton ratio is, and thus, gravitons have a greater number of inflatons from which they could scatter and deplete. Therefore, compared to the black hole description, the depletion in a corpuscular inflationary universe would be enhanced by a factor of N_ϕ/N. Since the slow-roll parameter can be related to the depletion rate of the condensate, an upper bound must be placed on the duration of inflation and, thus, on the number of e-foldings. This key result of corpuscular inflation indicates that the semi-classical approach cannot recover.

Additionally, this picture can shed light on the suitability of a de Sitter spacetime in describing inflationary cosmology. The exact de Sitter spacetime exists in the limit where $\epsilon = 0$. In this limit, the depletion rate of the background would diverge, and the condensate would decay instantly. Thus, the de Sitter description is inconsistent

with a slow-roll inflationary theory. Furthermore, the condition $\epsilon \neq 0$ places an upper bound on the duration of inflation and the number of e-folding. However, caution should be taken with this statement, as it does not apply to the efficacy of de Sitter as a descriptor of any cosmological scenario; the conclusion is solely that de Sitter spacetime does not hold in the slow-roll limit of inflation.

The following equation can describe corpuscular inflationary dynamics,

$$\frac{\dot{N}}{N} = H\left(\epsilon - \frac{1}{\sqrt{\epsilon}}\frac{1}{N}\right), \tag{4.11}$$

where the Hubble parameter is defined as, $H \equiv R_H^{-1}$. This equation encapsulates the background state's purely classical and corpuscular time evolution. The first term on the right-hand side of the equation, which survives the classical limit where $\hbar = 0$, describes the classical time evolution of the occupation number of gravitons due to the purely classical increase of the Hubble radius. The second term describes the quantum evolution of the condensate, i.e., its depletion; it asserts the upper bound on the duration of this epoch and excludes the de Sitter limit where $\epsilon = 0$. To explore this limit, one can consider the case where ϵ is arbitrarily small. While this is not necessarily a physically reasonable assumption, it serves to further define this upper bound. In this case, the first term of the above equation is negligible, and the evolution of N is purely quantum,

$$\dot{N}_{\text{quantum}} = -\frac{H}{\sqrt{\epsilon}} = -\frac{1}{\sqrt{N}\ell_p}\frac{N_\phi}{N}. \tag{4.12}$$

This is the equation for a black hole's depletion rate, given by equation (4.5), multiplied by an enhancement factor due to the presence of inflatons. The Hubble patch is analogous to a black hole with an enhanced depletion rate in a quantum-dominated regime. In this case, the number of e-folding cannot be computed solely from the slow-roll parameter, ϵ. Rather, the inflationary duration is given by the time it takes to deplete a number of quanta on the order of $1/N$. Taking H and ϵ as constant, the number of depleted quanta per Hubble time can be computed as,

$$\Delta N \equiv N_{\text{i}} - N_{\text{f}} = \frac{1}{\sqrt{\epsilon}}, \tag{4.13}$$

where N_i is the occupation number of the condensate at the beginning of inflation and N_f is the occupation number of the condensate at the end of inflation. Therefore, in this picture, the inflationary duration is given by $\mathcal{N}_{\text{quantum}} = N\sqrt{\epsilon}$. This is the time needed to deplete the entire reservoir, and it must be consistent with the classically evaluated number of e-foldings, leading one to the following consistency bound,

$$\epsilon > N^{-\frac{2}{3}}. \tag{4.14}$$

In the commonly assumed case of $V = m^2\phi^2$ inflation, where $\mathcal{N}_{\text{quantum}} = 1/\epsilon$, this condition can be written as,

$$\mathcal{N}_\epsilon < N^{\frac{2}{3}}. \tag{4.15}$$

This bound restricts how slow the potential could decrease, i.e., its concavity, and excludes any potential that leads to a positive cosmological constant. It can also be formulated in terms of the classical potential,

$$\left(\frac{M_{\text{Pl}}V'}{V}\right)^2 < \frac{1}{\hbar}\left(\frac{M_{\text{Pl}}^4}{V}\right)^{\frac{2}{3}}. \tag{4.16}$$

Evidently, the smaller the potential energy, the slower it is permitted to evolve (Dvali and Gomez 2014).

The remainder of this chapter will discuss an alternative theory of inflation that differs from the inflaton-driven model discussed previously. Inflation can also be modeled by a modified gravity theory, in which the action takes the form of,

$$S = \frac{1}{16\pi G}\int d^4x\sqrt{-g}f(R), \tag{4.17}$$

where $f(R) = \gamma\ell_p^2R^2$ and R is the Ricci scalar. This contribution of R^2 allows for an effective scalar degree of freedom or a scalar graviton that can drive the exponential inflationary expansion without an explicit inflaton field. In the corpuscular model, these scalar gravitons are a part of the composite background, and their interactions lead to the depletion of the condensate, which generates primordial perturbations.

4.2.2 Depletion

The remainder of this chapter will be spent computing the depletion rate of an inflationary patch. Before examining this computation, there are a few important remarks to keep in mind. Firstly, the corpuscular picture is valid within each Hubble patch of size L. To determine the total number of depleted gravitons in the universe after inflation, one must multiply the number in a single patch by the total number of such patches. Secondly, the number of gravitons, N, would remain constant only in an exact de Sitter space. Lastly, due to self-interaction, gravitons can be 'squeezed' out of their coherent ground state and become propagating perturbations. This process must satisfy the Wheeler-DeWitt constraint, which determines the occupation number of gravitons in a Hubble patch. Consequently, depletion is assumed to reduce N, and the final occupation number of propagating modes cannot exceed the initial number of background gravitons.

One can now begin by considering the classical background as a spatially flat FLRW metric,

$$ds^2 = -dt^2 + a^2(t)(dr^2 + r^2d\Omega^2). \tag{4.18}$$

The Friedmann equation can be gathered from the Hamiltonian constraint,

$$0 = \mathcal{H}_M + \mathcal{H}_G = 3H^2 - 8\pi G\rho, \tag{4.19}$$

where $\mathcal{H}_M \approx \rho$ is the matter-energy density and $\mathcal{H}_G$ is the analog for the graviton state given by the Einstein-Hilbert action,

$$S = \frac{1}{16\pi G}\int d^4x\sqrt{-g}R. \tag{4.20}$$

The Friedmann equation can be integrated over the volume contained within Hubble radius, L,

$$L^3H^2 \sim GL^3\rho \equiv GM_L. \tag{4.21}$$

The corpuscular description is recovered by quantizing M_L in units of Planck mass, $M_{\rm Pl}$.

$$N_L \sim \left(\frac{M_L}{M_{\rm Pl}}\right)^2, \tag{4.22}$$

where N_L is the number of composite quanta in each Hubble patch. Considering a de Sitter universe and equation (2.6), the Hubble radii can be defined as,

$$L = a\int \frac{dt}{a} = L_\Lambda \sim H_\Lambda^{-1}. \tag{4.23}$$

Consequently,

$$GM_L \sim L^3H^2 = L_\Lambda \sim H_\Lambda^{-1}. \tag{4.24}$$

These expressions are similar to that of a spherically symmetric black hole, just as Dvali and Gomez proposed.

The corpuscular model can be ascribed to a de Sitter spacetime by assuming the condensate can be characterized by a typical Compton length, $\lambda \approx L_\Lambda$, and thus, $M_\Lambda = N_\Lambda \ell_p M_{\rm Pl}/L_\Lambda$. Equation (4.24) then leads to the consistency condition for the graviton condensate,

$$\ell_p M_\Lambda \sim L_\Lambda M_{\rm Pl} \sim \sqrt{N_\Lambda}, \tag{4.25}$$

which implies that for a macroscopic universe $N_\Lambda \gg 1$. The de Sitter metric is recovered from a $f(R)$ theory of modified gravity where,

$$S = \frac{1}{16\pi G}\int d^4x\sqrt{-g}f(R), \tag{4.26}$$

and,

$$f(R) = \gamma\ell_p^2R^2, \tag{4.27}$$

where γ is a positive parameter. By varying the action, one can obtain the equation of motion,

$$6f'(R)H^2 = Rf'(R) - f(R) - 6H\dot{R}f''(R). \tag{4.28}$$

Given equation (4.27), this becomes,

$$12RH^2 = R^2 - 12H\dot{R}. \tag{4.29}$$

For de Sitter spacetime,

$$\dot{R} = 24H\dot{H} = 0, \tag{4.30}$$

$$\frac{R}{6} = \dot{H} + 2H^2 = 2H^2 = \frac{2\Lambda}{3}. \tag{4.31}$$

The left-hand side of this equation can be integrated over the Hubble radius, given by equation (4.24),

$$L_\Lambda^3 H_\Lambda^2 \approx L_\Lambda \equiv -GU_N. \tag{4.32}$$

Likewise, integrating the right-hand side of this equation leads to,

$$L_\Lambda^3 \left(\frac{\Lambda}{3}\right) \approx L_\Lambda \equiv GU_{PN}. \tag{4.33}$$

The Newtonian and post-Newtonian potential, U_N and U_{PN}, can now be introduced. Since there is no matter present in the universe under this model, the Hamiltonian becomes,

$$\mathcal{H}_G \approx U_N + U_{PN} = 0. \tag{4.34}$$

In the corpuscular description, the negative Newtonian energy of the condensate is explained by assuming each graviton has a negative binding energy, ϵ_Λ, given by the Compton relation. Thus, it takes the form of,

$$U_N \approx M_\Lambda \phi_N = N_\Lambda \epsilon_\Lambda = -N_\Lambda \frac{\ell_p M_{\rm Pl}}{L_\Lambda}. \tag{4.35}$$

The graviton self-interaction term gives the positive post-Newtonian energy,

$$U_{PN} \approx N_\Lambda \epsilon_\Lambda \phi_N = N_\Lambda^{3/2} \frac{\ell_p^2 M_{\rm Pl}}{L_\Lambda^2}, \tag{4.36}$$

where the Newtonian potential is given by,

$$\phi_N = -N_\Lambda \frac{\ell_p M_{\rm Pl}}{M_\Lambda L_\Lambda} = -\sqrt{N_\Lambda}\frac{\ell_p}{L_\Lambda}. \tag{4.37}$$

The gravitational Hamiltonian equation (4.34) can be expanded into two terms; one keeps track of its contribution to the Einstein-Hilbert action (4.20), while the other keeps track of its contribution to the effective action, (4.26). The latter takes the form of,

$$\mathcal{H}_G^{(2)} \approx \beta(U_N + U_{PN}) \approx 0, \tag{4.38}$$

where $\beta > 0$ to satisfy the consistency condition. The former takes the form of,

$$\mathcal{H}_G^{(1)} \approx \alpha U_N, \tag{4.39}$$

where $\alpha > 0$. Altogether, one finds,

$$\mathcal{H}_G = \mathcal{H}_G^{(1)} + \mathcal{H}_G^{(2)} \approx (\alpha + \beta)U_N + \beta U_{PN} = 0. \tag{4.40}$$

The term proportional to α indicates that an ideal de sitter condensate, described by (4.32) and (4.33), is not an adequate solution. For small departures from an ideal de Sitter scaling, the potential can take the form of,

$$G_N U_N \approx -L^3 H^2, \tag{4.41}$$

and,

$$G_N U_{PN} \approx L^3 L_\Lambda^{-2}, \tag{4.42}$$

where $L \approx L_\Lambda$ is the new Hubble radius. Equation (4.40) now yields,

$$L^3 \left[-(\alpha + \beta)H^2 + \beta L_\Lambda^{-2}\right] \approx 0, \tag{4.43}$$

where,

$$H^2 \approx \frac{\beta}{\alpha + \beta}\frac{1}{L_\Lambda^2}. \tag{4.44}$$

The de Sitter case is accurately reproduced when $\alpha = 0$; when $\alpha > 0$, $H < H_\Lambda$. If the system begins with $H \approx H_\Lambda$, then $\dot{H}$ must be negative to ensure that the constraint, (4.40), is satisfied at all times. This can be explicitly demonstrated by writing,

$$H = H_\Lambda + \dot{H}\delta t, \tag{4.45}$$

where the typical time scale is given by, $\delta t \approx L_\Lambda$, since gravitons with a Compton wavelength L_Λ are not sensitive to shorter times. Equation (4.43) ultimately yields,

$$\dot{H} \approx -\frac{\alpha}{\alpha + \beta}\frac{H_\Lambda}{\delta t} \approx -\frac{\alpha}{\alpha + \beta}\frac{1}{L_\Lambda^2}. \tag{4.46}$$

Furthermore, the slow-roll parameter in the corpuscular model is given by,

$$\epsilon \equiv -\frac{\dot{H}}{H^2} \approx \frac{\alpha}{\alpha + \beta}, \tag{4.47}$$

and one obtains $\epsilon = 0$, the exact de Sitter limit, when $\alpha \to 0$, neglecting quantum depletion.

Gravitons within the condensate generate the effective Hubble parameter $H \sim N_\Lambda^{-1/2} \sim L_\Lambda^{-1}$, but they also undergo scattering and depletion. Consequently, their occupation number changes over time according to

$$\ell_p \frac{\dot{N}_\Lambda}{\sqrt{N_\Lambda}} = \ell_p \frac{\dot{N}_\Lambda}{\sqrt{N_\Lambda}}\bigg|_{\text{classical}} + \ell_p \frac{\dot{N}_\Lambda}{\sqrt{N_\Lambda}}\bigg|_{\text{quantum}}, \tag{4.48}$$

where the classical equation of motion, where $\alpha \neq 0$, gives,

$$\ell_p \frac{\dot{N}_\Lambda}{\sqrt{N_\Lambda}}\bigg|_{\text{classical}} \approx -\frac{\dot{H}}{H^2} \approx \frac{\alpha}{\alpha+\beta} = \epsilon, \tag{4.49}$$

and the purely quantum depletion results in,

$$-\frac{\dot{H}}{H^2} = \ell_p \dot{M}_\Lambda \approx -\frac{M_{\text{Pl}}^2}{M_\Lambda^2} \approx -\ell_p^2 H^2 \approx -\frac{\beta}{\alpha+\beta}\frac{1}{N_\Lambda} \approx -\frac{1-\epsilon}{N_\Lambda}. \tag{4.50}$$

The positive contribution from equation (4.49) corresponds to a slowly growing Hubble patch, while the negative contribution from equation (4.50) corresponds to depletion and the generation of perturbations. Combining these two terms, one recovers a solution for the depletion rate of the condensate background,

$$-\frac{\dot{H}}{H^2} \approx \ell_p \frac{\dot{N}_\Lambda}{\sqrt{N_\Lambda}} \approx \epsilon\left(1 - \frac{\beta}{\alpha N_\Lambda}\right) \approx \epsilon - \frac{1-\epsilon}{N_\Lambda}, \tag{4.51}$$

leading to a critical value for α,

$$\alpha \gtrsim \alpha_c \approx \frac{\beta}{N_\Lambda} \sim \frac{\ell_p^2}{L_\Lambda^2}, \tag{4.52}$$

which can be interpreted as a minimum 'distance' from de Sitter.

One can consider this as the universe departing from de Sitter at $f(R) \approx R^2$ and asymptotically approaching a fixed point, $f(R) \approx R - \Lambda$, of general relativity, characterized by a positive cosmological constant. Assuming $R \approx \Lambda$ is constant (4.28) becomes,

$$6f'(R)H^2 \approx Rf'(R) - f(R). \tag{4.53}$$

Considering,

$$f(R) = \sum_{k=1}^{n} a_k \ell_p^{2k-2} R^k, \tag{4.54}$$

one can write,

$$Rf'(R) - f(R) = \sum_{k=2}^{n} (k-1) a_k \ell_p^{2k-2} R^k. \tag{4.55}$$

Equation (4.53) then becomes,

$$H^2\left(a_1 + \sum_{k=2}^{n} k a_k \ell_p^{2k-2} R^{k-1}\right) \approx \sum_{k=2}^{n} (k-1) a_k \ell_p^{2k-2} R^k. \tag{4.56}$$

Given, $R \approx \Lambda$ and $j = k-1$ one can find,

$$a_1 H^2 \approx \sum_{j=1}^{n-1} \left(\Lambda - H^2\right) j a_{j+1} \ell_p^{2j} \Lambda^j. \tag{4.57}$$

Considering equations (4.32) and (4.33),

$$H^2 \approx -\frac{G_N U_N}{L_\Lambda^3} \approx -\frac{\ell_p}{M_{\rm Pl} L_\Lambda^3} U_N, \tag{4.58}$$

$$\Lambda \approx \frac{G_N U_{PN}}{L_\Lambda^3} \approx \frac{\ell_p}{M_{\rm Pl} L_\Lambda^3} U_{PN}, \tag{4.59}$$

therefore,

$$a_1 U_N + (U_N + U_{PN}) \sum_{j=1}^{n-1} j a_{j+1} \left(\frac{\ell_p^3 U_{PN}}{L_\Lambda^3 M_{\rm Pl}} \right)^j \approx 0. \tag{4.60}$$

In the case of the Starobinsky potential, where n=2, one can write,

$$a_1 U_N + a_2 \left(\frac{\ell_p^3 U_{PN}}{L_\Lambda^3 M_{\rm Pl}} \right) (U_N + U_{PN}) \approx \alpha U_N + \gamma \frac{\ell_p^2}{L_\Lambda^2} (U_N + U_{PN}) \approx 0. \tag{4.61}$$

A comparison to equation (4.40) reveals,

$$\beta = \gamma \frac{\ell_p^2}{L_\Lambda^2}, \tag{4.62}$$

as expected during inflation.

4.2.3 Primordial Perturbations

This thesis focuses on the production of inflationary perturbations as described by the corpuscular model. Analogous to how Hawking radiation results from quantum depletion under a corpuscular description of a black hole, inflationary perturbations result from the quantum depletion of the background condensate under a corpuscular theory of inflationary cosmology. A factor of R^2 to the gravitational action gives rise to an effective scalar degree of freedom or a scalar graviton that, in the corpuscular model, is a part of the composite background. The scattering of these gravitons leads to their excitation and depletion, which is enhanced by inflatons. The excited inflatons that escape the condensate result in scalar perturbations that produce density fluctuations; the excited gravitons that escape result in tensor perturbations that produce gravitational waves. This depletion process is also responsible for 'turning off' inflation; once depletion is no longer energetically favorable, inflation ends. It is important to note that in contrast to the semi-classical theory, quanta production is not a vacuum process. Additionally, the excited quanta do not affect the dynamics of the background. In other words, the back-reaction of scalar and tensor perturbations is negligible. As previously stated, this model has two species of quanta at play: gravitons and inflatons. Therefore, there are three types of interactions to consider: graviton-graviton, (g-g), graviton-inflaton, (g-ϕ), and inflaton-inflaton, (ϕ-ϕ). ϕ-ϕ processes are negligible as their wavelength is virtually infinite in the slow-roll regime. g-ϕ and g-g scatters differ by a combinatorial

factor, N_ϕ, where $N_\phi \gg N$. Therefore, g-ϕ processes dominate, and gravitons and inflatons deplete at the same rate. Lastly, as shown by (4.48), the rate of change of the number of composite quanta has both a classical contribution and a quantum contribution (Casadio, Kühnel, and Orlandi 2015).

Chapter 5

Perturbations from Depletion

This chapter will report the findings computed throughout this thesis project. The occupation number of primordial perturbations will be derived within a corpuscular framework. The computed value will be compared to the quantum field theory result to analyze its efficacy. This computation will first be conducted assuming a toy model in which the occupation number of constituent quanta is constant. Then, a time-dependent occupation number will be considered. Subsequently, a time-dependent slow-roll parameter, ϵ, will be considered. The number of quanta depleted by each inflationary de Sitter patch will be derived. A discussion on the number of de Sitter patches and the impact of the number of species of constituent quanta will follow this.

5.1 Occupation Number of Depleted Quanta

The occupation number of depleted quanta can be computed by performing a time integration over the depletion rate derived in the previous chapter. This depletion rate can be initially computed assuming a toy model in which the occupation number of constituent quanta, N_Λ, is constant in time. Subsequently, a derivation considering a time-dependent N_Λ will be provided. Lastly, the final result for the occupation number of depleted quanta is computed considering both a time-dependent N_Λ and slow-roll parameter, ϵ. This result shows that the number of depleted quanta can be explicitly related to the number of e-folding and the Hubble parameter at the beginning and end of inflation.

5.1.1 Computing N_k using a Toy-Model

To assess the number of primordial perturbations under the corpuscular model, one can consider perturbations with wave number, k, that exit the Hubble horizon once their wavelength reaches $\lambda \approx a_{out}/k \approx L_\Lambda$, and re-enter the Hubble horizon

when $\lambda \approx a_{in}/k$. Depending on whether the reentry occurred during the radiation-dominated or matter-dominated era, the wavelength of these perturbations at the moment of re-entry is approximately L_{rad} or L_{dust}. These modes, considered to be initially empty, become occupied outside the horizon. The occupation number computed in Chapter 3 under the semi-classical approach is given by,

$$N_k \simeq e^{\sigma \mathcal{N}_k}, \tag{5.1}$$

where,

$$e^{\mathcal{N}_k} = \frac{a_{\rm in}}{a_{\rm out}}. \tag{5.2}$$

The parameter σ is a coefficient of the order one. It can be adjusted to ensure the compatibility of the quantum field theory (QFT) result (5.1) with the corpuscular model. Under the corpuscular model, the time evolution of the composite background can be written as,

$$\frac{\ell_p \dot{N}_\Lambda}{\sqrt{N_\Lambda}} \simeq \epsilon - \frac{1-\epsilon}{N_\Lambda}, \tag{5.3}$$

where, $N_\Lambda = N_\Lambda(t)$ is the number of gravitons in the background condensate. Furthermore, the time evolution of the depleted quanta can be described as,

$$\frac{\ell_p \dot{N}_k}{\sqrt{N_\Lambda}} \simeq \frac{1-\epsilon}{N_\Lambda}. \tag{5.4}$$

One can begin by considering a toy model where $\dot{N}_\Lambda = 0$; equation (5.3) simplifies to,

$$0 \simeq \epsilon - \frac{1-\epsilon}{N_\Lambda}, \tag{5.5}$$

$$N_\Lambda = \frac{1-\epsilon}{\epsilon}. \tag{5.6}$$

Thus, equation (5.4) becomes,

$$\dot{N}_k = \frac{(\epsilon - \epsilon^2)^{\frac{1}{2}}}{\ell_p}. \tag{5.7}$$

This equation can be integrated and compared to equation (5.1); assuming a constant ϵ,

$$N_k = \int_{t_{out}}^{t_{in}} \dot{N}_k \, dt = \int_{t_{out}}^{t_{in}} \frac{(\epsilon - \epsilon^2)^{\frac{1}{2}}}{\ell_p} \, dt = \frac{(\epsilon - \epsilon^2)^{\frac{1}{2}}}{\ell_p}(t_{in} - t_{out}) \tag{5.8}$$

The value of the slow-roll parameter, ϵ, can be approximated from CMB observables. The scalar spectral index can be related to the slow-roll parameters by (Baumann 2012),

$$n_s - 1 = 2\eta - 6\epsilon. \tag{5.9}$$

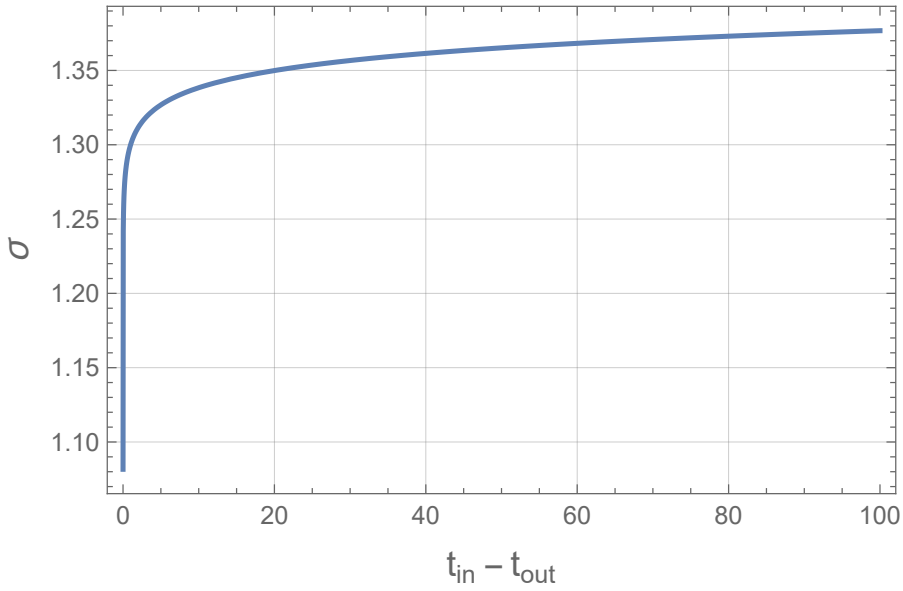

Figure 5.1: Plot of the parameter σ as a function of $t_{in} - t_{out}$; as given by $\sigma \approx 1.3 + \ln(t_{in} - t_{out})/60$. It should be noted that $\sigma \geq 1$ always; therefore, this solution is compatible with the QTF result, $N_k \simeq e^{\sigma \mathcal{N}_k}$.

The most recent Plank measurements of CMB anisotropies found $n_s = 0.965 \pm 0.004$ (Aghanim et al. 2020). Assuming a quadratic inflationary potential, where $\eta \approx \epsilon$, we can find $\epsilon \approx 10^{-2}$. As $\ell_p \approx 10^{-35}$m, N_k can be written as,

$$N_k = 10^{34}(t_{in} - t_{out}). \tag{5.10}$$

This solution can now be compared to equation (5.1), and thus σ can be written as,

$$\sigma \approx \frac{1}{\mathcal{N}_k} \ln(10^{34}(t_{in} - t_{out})). \tag{5.11}$$

Assuming $\mathcal{N}_k \approx 60$ this equation becomes,

$$\sigma \approx 1.3 + \frac{\ln(t_{in} - t_{out})}{60}. \tag{5.12}$$

This can be visualized by Figure 5.1, a plot of σ against $t_{in} - t_{out}$, the duration the perturbation spends outside the horizon. From this, one can assess if this model produces physically reasonable solutions for σ. Moreover, as this graph reflects $\sigma \geq 1$ for all σ and as $\mathcal{N}_k$ must be at least 60, N_k must always be greater than one. Therefore, this overly simplistic corpuscular model is consistent with the standard cosmological model.

5.1.2 Computing N_k considering $N_\Lambda = N_\Lambda(t)$

The occupation number of constituent gravitons decreases throughout inflation. Therefore, utilizing a time-dependent N_Λ allows for a more accurate assessment

of the value of N_k. Consider $N_\Lambda(t_{out}) \simeq {L_\Lambda}^2/{\ell_p}^2 \simeq (1/H\ell_p)^2$, where $L_\Lambda \simeq H^{-1}$. Equation (5.4) becomes,

$$\dot{N}_k = (1-\epsilon)H. \tag{5.13}$$

Now, one can integrate over time to find N_k,

$$\begin{aligned} N_k(t_{out}) &= \int_{t_{out}}^{t_{in}} \dot{N}_k(t_{out})\, dt \\ &= (1-\epsilon)\int_{t_{out}}^{t_{in}} H(t)\, dt \\ &= (1-\epsilon)\ln\left(\frac{a_{in}}{a_{out}}\right) \\ &= (1-\epsilon)\mathcal{N}_k. \end{aligned} \tag{5.14}$$

This result should equal (5.1). The dependence of a on k is given by the horizon crossing condition, $k = aH$. Furthermore, the dependence of σ on k is manifest, and the value of $\sigma = \sigma_k$ can be found from the value of ϵ given by the scalar spectral index. To find $\sigma = \sigma_k$ one can set equation (5.1) equal to equation (5.14),

$$N_k = (1-\epsilon)\mathcal{N}_k = e^{\sigma\mathcal{N}_k}. \tag{5.15}$$

Thus,

$$e^{\sigma} = (1-\epsilon)\mathcal{N}_k e^{-\mathcal{N}_k}, \tag{5.16}$$

$$\sigma_k = \ln(1-\epsilon) + \ln(\mathcal{N}_k) - \mathcal{N}_k. \tag{5.17}$$

Given the observed value of ϵ and equation (5.17), σ can be plotted as a function of the number of e-folds, seen by Figure 5.2. These results show that σ must always be negative while $\mathcal{N}_k$ must always be positive. This is consistent with the requirement that the number of e-folding must be at least 60 to resolve the problems associated with the Hot Big Bang model. However, complications arise in its comparison to equation (5.1). These results indicate that the occupation number of perturbations must be between 0 and 1, which is physically unreasonable. Furthermore, if N_k is less than 1 and $\mathcal{N}_k = 60$ then equation (5.14) indicates that ϵ must be greater than 59/60, which is inconsistent with the observed value of $\epsilon \approx 10^{-2}$. This inconsistency can be attributed to a time-independent ϵ assumption. In reality, ϵ grows until it is equal to 1 at the end of inflation, which occurs at t_{end} between t_{in} and t_{out}, thus $\epsilon = \epsilon(t)$.

5.1.3 Computing N_k considering $N_\Lambda = N_\Lambda(t)$ and $\epsilon = \epsilon(t)$

A time-dependent ϵ can be defined by,

$$\epsilon \equiv -\frac{\dot{H}}{H^2}. \tag{5.18}$$

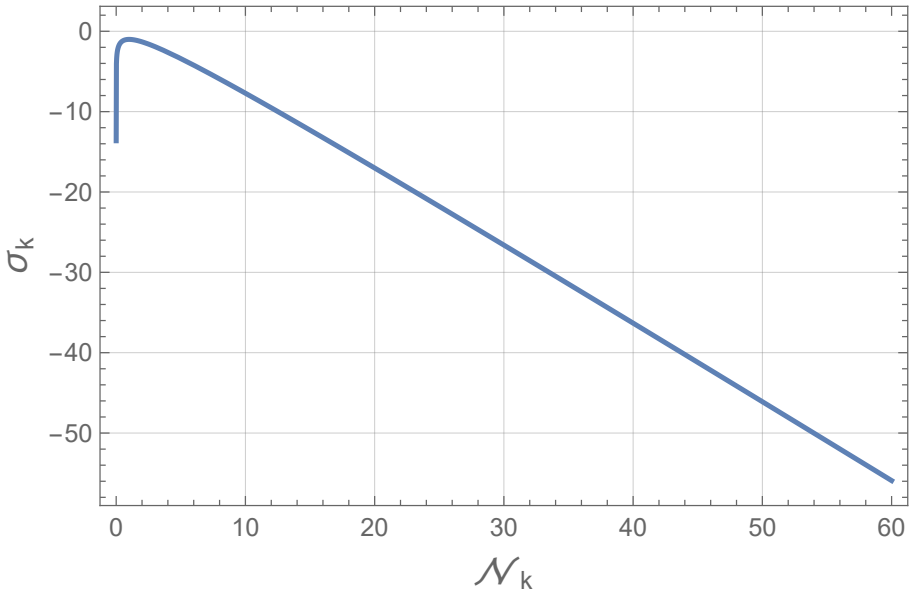

Figure 5.2: Plot of $\sigma_k = ln(1-\epsilon) + \ln(\mathcal{N}_k) - \mathcal{N}_k$, where $\epsilon = 10^{-2}$. This plot shows a critical point where $\sigma = -1$ and $\mathcal{N}_k = 1$, providing an upper bound on σ, following this point σ remains inversely proportional to $\mathcal{N}_k$. It should be noted that $\sigma < 0$ always; therefore, this solution is not compatible with the QTF result, $N_k \simeq e^{\sigma \mathcal{N}_k}$.

Therefore, N_k can be written as,

$$N_k = \int_{t_{out}}^{t_{in}} (1-\epsilon(t))H(t)\,dt = (1-\epsilon)\int_{t_{end}}^{t_{in}} H(t)\,dt + \int_{t_{out}}^{t_{end}} (1-\epsilon(t))H(t)\,dt. \quad (5.19)$$

However, as $\epsilon = 1$ by the end of inflation, the first term cancels,

$$\begin{aligned} N_k &= \int_{t_{out}}^{t_{end}} (1-\epsilon(t))H(t)\,dt \\ &= \int_{t_{out}}^{t_{end}} H(t)\,dt - \int_{t_{out}}^{t_{end}} \epsilon(t)H(t)\,dt \\ &= \ln\frac{a_{end}}{a_{out}} - \int_{t_{out}}^{t_{end}} \epsilon(t)H(t)\,dt. \end{aligned} \quad (5.20)$$

Considering equation (5.18),

$$\begin{aligned} N_k &\approx \ln\frac{a_{end}}{a_{out}} + \int_{t_{out}}^{t_{end}} \frac{\dot{H}(t)}{H^2(t)} H(t)\,dt \\ &\approx \ln\frac{a_{end}}{a_{out}} + \int_{t_{out}}^{t_{end}} \frac{\dot{H}(t)}{H(t)}\,dt \\ &\approx \ln\frac{a_{end}}{a_{out}} + \ln\frac{H_{end}}{H_{out}} \\ &\approx \ln\frac{a_{end}}{a_{out}}\frac{H_{end}}{H_{out}} \\ &\approx \boxed{\mathcal{N}_k \ln\frac{H_{\rm end}}{H_{\rm out}}}. \end{aligned} \quad (5.21)$$

As,

$$H_{end} > H_{out}, \tag{5.22}$$

N_k will always be positive. Therefore, the inconsistency of the previous solution given by equation (5.14) is remedied, and the above solution is compatible with the QFT result. However, the magnitude of depleted quanta given by this result is insufficient to reproduce the magnitude of primordial perturbations evidenced by CMB anisotropies.

5.2 Channels and Patches

This section will provide a physical interpretation of the results of the previous section and discuss some possible amendments that should be considered. The number of depleted quanta computed in the previous section holds for each inflationary patch. Thus, it must be multiplied by the number of patches to reproduce the number of primordial perturbations evidenced by the CMB. Furthermore, according to corpuscular theory, the depletion rate is enhanced by the number of species of constituent quanta. Therefore, the number of depleted quanta previously computed should be multiplied by the number of polarization states of the constituent gravitons.

5.2.1 Multiple de Sitter Patches

To remedy this inconsistency, one must understand the physical interpretation of the QFT result. The semi-classical view of inflation proposes that each inflationary de Sitter patch grows by a factor of $e^{\mathcal{N}}$, where $\mathcal{N}$ is the number of e-folding and is approximately 60. In the corpuscular model, the universe at the end of inflation can be described by $e^{\mathcal{N}}$ overlapping de Sitter patches. Therefore, the total number of depleted wave modes would be equal to (5.21) times $e^{\mathcal{N}}$. Thus, the magnitude of (5.21) is inconsistent because this formula defines the number of depleted quanta given by each de Sitter patch. The corpuscular result must be multiplied by the number of de Sitter patches to compare it to CMB observations. Therefore, the total number of depleted wave modes is given by,

$$N_{tot} \approx e^{\mathcal{N}} \mathcal{N} \ln \frac{H_{\text{end}}}{H_{\text{out}}}. \tag{5.23}$$

Moreover, this analysis sheds light on the physical interpretation of σ in (5.1); it accounts for the number of inflationary de Sitter patches.

5.2.2 Multiple Depletion Channels

This addendum to the solution (5.21) can be further refined by considering multiple depletion channels. The number of species of quanta enhances the rate of depletion as each species gives way to a new depletion channel. Therefore, the number of predicted depleted quanta should be multiplied by the number of species of quanta. The corpuscular model assumes the background condensate is composed of two species of quanta: inflatons and gravitons. Depletion is dominated by inflaton-graviton scattering; however, the two polarizations of gravitons could enhance the number of depletion channels. Inflatons are spin-0 particles that lack intrinsic polarizations (Dvali and Gomez 2014). Gravitons have helicity ± 2 corresponding to '+' and 'x' polarizations (Palmerduca and Qin 2024). Inflaton-graviton scattering dominates depletion, and considering two species of gravitons, the number of quanta each channel depletes sum to give the total depletion,

$$N_{k,tot} = N_{k,g_+} + N_{k,g_x}. \tag{5.24}$$

where N_{k,g_+} is the number of depleted quanta due to inflaton- '+' graviton scatters and N_{k,g_x} is the number of depleted quanta due to inflaton- 'x' graviton scatters. Assuming $\lambda_{k,g_+} \approx \lambda_{k,g_x}$,

$$N_{k,g_+} \approx N_{k,g_x}. \tag{5.25}$$

Therefore, equation (5.23) becomes,

$$N_{tot} \approx 2e^{\mathcal{N}}\mathcal{N} \ln \frac{H_{\text{end}}}{H_{\text{out}}}, \tag{5.26}$$

which differs from the previous result by a factor of two. While a factor of 2 is likely not very cosmologically significant, the relation between the depletion rate and the number of constituent species is an interesting phenomenon to remember when discussing corpuscular inflation.

Chapter 6

Discussion and Conclusion

This thesis has focused on analyzing the corpuscular model applied to an inflationary universe. Inflation, typically described with a semi-classical approach, is the rapid exponential expansion theorized to occur in the first fraction of a second after the Big Bang. While there is broad consensus that such a period is needed to remedy key issues with the Hot Big Bang model, such as the Horizon, Flatness, and Monopole problems, it is notoriously difficult to study. This difficulty arises from modern cosmology's limited theoretical consensus and observational capacity.

Theoretically, the standard cosmological model has several limitations that hinder scientific consensus. Inflation is considered to be driven by a hypothetical scalar field called the inflaton; however, little is known about the exact nature of this field and how it fits into Standard Model physics. Additionally, the study of inflation requires a knowledge of physics near the Planck scale, i.e., a theory of quantum gravity, for which there is little scientific consensus. In other words, one of the most significant limitations of the semi-classical theory of inflation is its inability to reconcile the quantum nature of the space-time background and the back-reaction of primordial perturbations on that background. Another critique of semi-classical inflationary theory is that it requires the inflationary universe to follow the slow-roll trajectory, i.e., maintaining slow-roll conditions until the end of inflation, at which point these conditions are violated. However, it does not explain why the universe would follow such a trajectory.

From an observational perspective, the empirical evidence used to study inflation is limited, as is the prospect of experimental corroboration. The key inflationary observable is the CMB. While a wealth of information is imprinted into the CMB, the semi-classical approach views it as merely a snapshot of the universe at the end of inflation; therefore, it does not store information throughout inflation. Furthermore, inflationary conditions cannot be reproduced in a lab as the energy scales of the universe at this time are near the GUT scale; such scales are too high for particle accelerator experiments.

A corpuscular description can remedy many of these constraints with the semi-classical picture. Corpuscular cosmology replaces the classical curved background metric with a quantum composite background. In this scenario, the wavelength of quanta is set by the 'would be' classical curvature metric and classical geometry is recovered at the limit where the occupation number of the composite state, N, approaches infinity. While this model was first applied to black holes, it can be extended to all maximally symmetric spaces, such as the inflationary universe. In this description, the inflationary universe acts as a Bose-Einstein condensate.

Theoretically, the corpuscular model can fill in many gaps left open by the semi-classical model. The corpuscular model provides a foundation for holography; when this picture is applied to AdS space, the occupation number of gravitons correlates to the central charge of a CFT. Additionally, the corpuscular model puts forth an alternative explanation for particle creation. While the semi-classical model assumes particle creation is a vacuum process, the corpuscular model attributes this to condensate depletion, i.e., the scattering of constituent off-shell quanta. Only in the limit where the occupation number, N, approaches infinity can this be confused for a vacuum process.

This should not be overlooked as it has broad implications for both the theoretical and observational studies of inflationary cosmology. Explaining particle production as purely a vacuum process leads to difficulties in addressing the extent of reheating and the back-reaction of particle production on inflationary dynamics. Additionally, this alternative explanation for Hawking radiation has several implications for black hole physics; for example, it would provide a solution to the information paradox. Moreover, particle creation via depletion broadens the capacity for observational and experimental studies. Under this model, the CMB does not merely contain information on the state of the universe at the end of inflation; instead, it stores the cumulative effects of depletion throughout the entire duration of inflation. Additionally, while particle accelerators cannot reproduce inflationary conditions, the depletion of Bose-Einstein condensates can be studied in a laboratory.

The occupation number of depleted quanta computed in this project provides a basis for further research to corroborate the corpuscular model with observations. The primordial density fluctuations imprinted in the CMB result from the depletion of the condensate background. Therefore, the amplitude of primordial density fluctuations in the CMB can be compared to the occupation number of depleted quanta computed in this paper to check this model's compatibility with cosmological observations.

This paper discussed the key inflationary observable, the Cosmic Microwave Background. The formation of the CMB, as well as the statistical information it carries, was discussed. Subsequently, the Hot Big Bang model was introduced, as

were its limitations, the flatness, horizon, and monopole problems. It was then explained how a period of rapid accelerated expansion, known as inflation, can solve these problems. Furthermore, the conditions such a period is required to meet, namely the slow-roll conditions, were explored. Chapter 2 concluded with a discussion on slow-roll inflationary dynamics.

Chapter 3 focused on primordial perturbations under a semi-classical framework, resulting from quantum fluctuations in the classical inflaton field. It began by discussing the formation and evolution of these perturbations during inflation. These fluctuations were then quantized to calculate their power spectrum. The theoretical inflationary phase, in which the production of perturbations grows exponentially, known as the ultra-slow roll phase, was then discussed. This was followed by a derivation of the occupation number of inflationary perturbations using quantum field theory. This result is later compared with the analogous corpuscular result in Chapter 5.

Up to this point, inflation was discussed with a semi-classical approach. In Chapter 4, the focus shifted to a purely quantum, corpuscular model of cosmology. This model was first applied to black holes, and this prescription was briefly discussed. This prescription was then generalized to all maximally symmetric cosmological spaces. This framework was then used to address inflationary dynamics in a corpuscular model. Here, the generation of primordial perturbations is interpreted as the depletion of the background condensate. Thus, the occupation number of inflation perturbations could be computed by integrating the depletion rate of the background. The derivation of this depletion rate was provided, setting the stage for the final computation in the next chapter.

This project aimed to compute the occupation number of depleted quanta under a corpuscular inflationary model. Stemming from the works of (Dvali and Gomez 2014) and (Casadio, Kühnel, and Orlandi 2015), this paper computed the occupation number of depleted quanta by integrating over the depletion rate computed in previous works. This value was then compared to the QFT result for primordial perturbations to assess its feasibility. The number of depleted modes was recovered for each inflationary de Sitter patch. It can be multiplied by the number of patches to recover the magnitude of density fluctuations imprinted in the CMB. Further refinement of this picture can be given by accounting for the multiple polarization states of the composite gravitons. Each additional species in the condensate gives way to an additional depletion channel. Therefore, the number of depleted quanta computed should be multiplied by the number of constituent species. The results of this thesis indicate that the corpuscular theory can produce physically reasonable values for the number of primordial perturbations and, thus, the number of

e-folding. The next step would be to directly compare the occupation number computed in the previous chapter to the amplitude of the power spectrum of primordial perturbations given by the CMB. The findings presented in this thesis, and those made by corpuscular theory as a whole, show that thus far, the corpuscular theory can recover the observational findings of the standard semi-classical inflation model.

Bibliography

Aghanim, N. et al. (Sept. 2020). "Planck2018 results: VI. Cosmological parameters". In: *Astronomy amp; Astrophysics* 641, A6. ISSN: 1432-0746. DOI: 10.1051/0004-6361/201833910. URL: http://dx.doi.org/10.1051/0004-6361/201833910.

Akrami, Y. et al. (Sept. 2020). "Planck2018 results: IV. Diffuse component separation". In: *Astronomy amp; Astrophysics* 641, A4. ISSN: 1432-0746. DOI: 10.1051/0004-6361/201833881. URL: http://dx.doi.org/10.1051/0004-6361/201833881.

Ballesteros, Guillermo et al. (July 2020a). "Primordial black holes as dark matter and gravitational waves from single-field polynomial inflation". In: *Journal of Cosmology and Astroparticle Physics* 2020.07, pp. 025–025. ISSN: 1475-7516. DOI: 10.1088/1475-7516/2020/07/025. URL: http://dx.doi.org/10.1088/1475-7516/2020/07/025.

— (Aug. 2020b). "Stochastic inflationary dynamics beyond slow-roll and consequences for primordial black hole formation". In: *Journal of Cosmology and Astroparticle Physics* 2020.08, pp. 043–043. ISSN: 1475-7516. DOI: 10.1088/1475-7516/2020/08/043. URL: http://dx.doi.org/10.1088/1475-7516/2020/08/043.

Baumann, Daniel (2012). *TASI Lectures on Inflation*. arXiv: 0907.5424 [hep-th]. URL: https://arxiv.org/abs/0907.5424.

Casadio, Roberto, Florian Kühnel, and Alessio Orlandi (Sept. 2015). "Consistent cosmic microwave background spectra from quantum depletion". In: *Journal of Cosmology and Astroparticle Physics* 2015.09, pp. 002–002. ISSN: 1475-7516. DOI: 10.1088/1475-7516/2015/09/002. URL: http://dx.doi.org/10.1088/1475-7516/2015/09/002.

Coles, Peter and Francesco Lucchin (2002). *Cosmology: The Origin and Evolution of Cosmic Structure*. 2nd. Chichester, England: Wiley. ISBN: 0-471-48909-3.

Dvali, Gia and Cesar Gomez (2011). *Black Hole's Quantum N-Portrait*. arXiv: 1112.3359 [hep-th]. URL: https://arxiv.org/abs/1112.3359.

— (2012). *Black Holes as Critical Point of Quantum Phase Transition*. arXiv: 1207.4059 [hep-th]. URL: https://arxiv.org/abs/1207.4059.

— (Jan. 2014). "Quantum compositeness of gravity: black holes, AdS and inflation". In: *Journal of Cosmology and Astroparticle Physics* 2014.01, pp. 023–023. ISSN: 1475-7516. DOI: 10.1088/1475-7516/2014/01/023. URL: http://dx.doi.org/10.1088/1475-7516/2014/01/023.

Fixsen, D. J. (Nov. 2009). "THE TEMPERATURE OF THE COSMIC MICROWAVE BACKGROUND". In: *The Astrophysical Journal* 707.2, pp. 916–920. ISSN: 1538-4357. DOI: 10.1088/0004-637x/707/2/916. URL: http://dx.doi.org/10.1088/0004-637X/707/2/916.

Guth, Alan H. (Jan. 1981). "Inflationary universe: A possible solution to the horizon and flatness problems". In: *Phys. Rev. D* 23 (2), pp. 347–356. DOI: 10.1103/PhysRevD.23.347. URL: https://link.aps.org/doi/10.1103/PhysRevD.23.347.

Palmerduca, Eric and Hong Qin (2024). *Graviton topology*. arXiv: 2404.11696 [math-ph]. URL: https://arxiv.org/abs/2404.11696.

Vazquez Gonzalez, J. Alberto, Luis E. Padilla, and Tonatiuh Matos (Jan. 2020). "Inflationary cosmology: from theory to observations". In: *Revista Mexicana de Física E* 17.1 Jan-Jun, pp. 73–91. ISSN: 1870-3542. DOI: 10.31349/revmexfise.17.73. URL: http://dx.doi.org/10.31349/RevMexFisE.17.73.